JAERI-M
91-194

CONCEPTUAL DESIGN OF FUSION EXPERIMENTAL REACTOR

(FER/ITER)

— ELECTRON CYCLOTRON WAVE SYSTEM —

November 1991

Takumi YAMAMOTO, Masaki TUNEOKA, Keishi SAKAMOTO
Haruyuki KIMURA, Takashi NAGASHIMA, Koichi MAKI, Yasushi SAITOH*
Tadao OHNO* and Yasuyuki ITOH*

日本原子力研究所
Japan Atomic Energy Research Institute

JAERI-Mレポートは，日本原子力研究所が不定期に公刊している研究報告書です。
入手の問合わせは，日本原子力研究所技術情報部情報資料課（〒319-11茨城県那珂郡東海村）あて，お申しこしください。なお，このほかに財団法人原子力弘済会資料センター（〒319-11 茨城県那珂郡東海村日本原子力研究所内）で複写による実費頒布をおこなっております。

JAERI-M reports are issued irregularly.
Inquiries about availability of the reports should be addressed to Information Division Department of Technical Information, Japan Atomic Energy Research Institute, Tokai-mura, Naka-gun, Ibaraki-ken 319-11, Japan.

編集兼発行　日本原子力研究所
印　　刷　いばらき印刷㈱

JAERI-M 91-194

Conceptual Design of Fusion Experimental Reactor (FER/ITER) - Electron Cyclotron Wave System -

Takumi YAMAMOTO, Masaki TUNEOKA[+], Keishi SAKAMOTO[+]
Haruyuki KIMURA[++], Takashi NAGASHIMA[+], Koichi MAKI[++]
Yasushi SAITOH[*], Tadao OHNO[*] and Yasuyuki ITOH[*]

Department of Fusion Facility
Naka Fusion Research Establishment
Japan Atomic Energy Research Institute
Naka-machi, Naka-gun, Ibaraki-ken

(Received October 15, 1991)

Conceptual design of Electron Cyclotron Wave (ECW) system for FER has been conducted, considering advanced physics and technological requirements. 20 MW and 140 GHz ECW system, providing strong electron heating at the core plasma as well as assist of plasma current initiation, is considered. Japanese contribution to the conceptual design of ECW system for ITER is also presented.

Keywords: ECH, FER, ITER, Conceptual Design

+ Department of Fusion Engineering Research
++ Fusion Experimental Reactor Team
* Toshiba Corporation

核融合実験炉（FER/ITER）の概念設計
－電子サイクロトロン波システム－

日本原子力研究所那珂研究所核融合装置試験部
山本　巧・恒岡まさき[+]・坂本　慶司[+]・木村　晴行[++]
永島　孝[+]・真木　紘一[++]・斉藤　靖[*]・大野　忠男[*]
伊藤　保之[*]

（1991年10月15日受理）

FERのための電子サイクロトロン波システムの物理的仕様と技術的な可能性を検討して，概念設計を行った。プラズマ中心の高電力密度電子加熱及びプラズマ電流立ち上げの高性能化として，20MW，140GHzの電子サイクロトロン波システムを検討した。また，ITERの電子サイクロトロン波システムの概念設計に対する日本貢献について述べる。

那珂研究所：〒311-01　茨城県那珂郡那珂町大字向山801-1
＋　核融合工学部
＋＋　核融合実験炉特別チーム
＊　東芝

Contents

目　　次

1. INTRODUCTION

1.1 Concepts of FER and ITER

JAERI has performed conceptual design of the fusion experimental reactor in both domestic and international cooperation programme for these three years. Fusion Experimental Reactor (FER)[1] corresponds to the domestic program. Basic objectives of FER are to explore a machine that solves reasonable minimum physical and technological issues necessary to proceed to a demonstration power reactor (DEMO) without any further intermediate steps. Achievement of Q (energy multiplication factor)~ 20 and steady state at least separately under well controlled conditions are considered to be a reasonable step to build the DEMO. International Thermonuclear Experimental Reactor (ITER) [2] also corresponds to the international cooperation program, where four parties (EURATOM, Japan, the Soviet Union and the United States) join under the auspices of IAEA. Major objectives of ITER are as follows: (1) to demonstrate controlled ignition and extended burn of D-T plasma, with steady state as an ultimate goal, (2) to demonstrate technologies essential to a reactor in an integrated system and (3) to perform integrated testing of the high-heat-flux and nuclear components required to utilize fusion power.

Major machine and plasma parameters for FER and ITER are as follows:

	FER	ITER
Major radius (m)	4.7	6.0
Minor Radius (m)	1.6	2.15
Elongation	2.0	2.0
Toroidal field (T)	5.25	4.85
Plasma current (MA)	15	22
Fusion power (GW)	0.6	1.0

1.2 Heating and Current Drive Scenarios of FER and ITER

Roles of heating and current drive system necessary for operations of FER/ITER are considered as follows [3]:

(1) Ionization, Preheating, and Current Initiation

(2) Non-inductive Current Ramp-up Assist

(3) Heating to Ignition

(4) Steady-state Current Drive

(5) Local Current Profile Control

(6) Burn Control

As it is difficult to cover all these functions by any single heating and current drive system, combination of plural systems is inevitable. Following four heating and current drive systems were thought as the candidates.

(1) Neutral Beam (NB) System

(2) Ion Cyclotron Wave (IC) System

(3) Lower Hybrid Wave (LH) System

(4) Electron Cyclotron Wave (EC) System

Selection was made from the experimental database obtained before and during the conceptual design phase and from modeling calculations.

For FER, 50 MW, 0.5 MeV NB is selected as main current drive and heating system, since some database exists for the current drive [4-6] and then a theoretical current drive efficiency shows the best value among all schemes for FER/ITER plasma. 30 MW, 5 GHz LH system is also selected for current ramp-up assist and current drive in the outer region of the plasma. A plenty of the database on the current drive by LH waves have been established in many tokamaks. A record value of the current drive figure of merit (γ) of 0.34×10^{20} Am^{-2} W^{-1} was obtained on JT-60.[7] However, in the steady-state scenario of FER/ITER, a driven current channel by the LH waves will be limited in the outer region because of a high electron temperature (volume-averaged electron temperature $\langle Te \rangle \sim$ 20 keV). Current profile control can be also expected in combination of NB and LH current drives in order to obtain stable plasma at high-β and to avoid the sawtooth oscillation. In addition, Volts•sec saving by LHCD [8] in the current ramp-up phase is quite useful to get higher plasma current or longer pulse discharge in FER, whose magnetic flux of the ohmic coil is relatively small. Thus the combination of NB and LH systems at total power of 80 MW has been chosen for the heating and current drive system of FER.

In order to supplement a central heating capability, either 20 MW, 50-85 MHz IC system or 20 MW, 140 GHz EC system were considered. With IC system, unique central ion heating can be expected. This capability is favorable for getting high Q and for burn control, even at high electron density, at which penetration of NB to the plasma center tends to be difficult. With EC system, strong central electron heating is possible. In addition, EC system is a powerful tool for the preionization and the current initiation. If IC system will be chosen as a central heating method, a short pulse (< 1 sec), several MW EC system will be necessary for the preionization and the current initiation. Stabilization and control of the sawtooth oscillation can be expected with both IC and EC systems.

For ITER, following two options have been determined in the course of the Conceptual Design Activity (CDA).

Reference: 75 MW, 1.3 MeV NB System
50 MW, 5 GHz LH System
20 MW, 120 GHz EC System

Alternate: 130 MW, 15-80 MHz IC System
50 MW, 5 GHz LH System
20 MW, 120 GHz EC System

A reason why the combination of NB and LH systems is employed as the reference scenario for current drive and heating is the same as for FER, but EC system is included in the reference scenario. Role of EC system is partly different from that of FER. Capability of local current profile control near q=2 magnetic surface for the purpose of avoidance of disruptions is added instead of the central heating as considered for FER. In the alternative scenario, IC system replaces NB system. A reason why IC system is not chosen as a reference system is its sparse database on the current drive and its lower theoretical current drive efficiency (about two third of NBCD efficiency). However, it has been proposed that both NB and IC should be part of the reference system from a point of view of considering merits of IC system (unrivaled central ion heating, unnecessity of a large scale engineering development and low cost). This point will be discussed in the coming Engineering Design Activity (EDA).

1.3 Electron Cyclotron Wave system for FER and ITER

In this report, the conceptual design of EC wave system is discussed mainly for FER and Japanese contribution to ITER EC system is described. The system for FER is basically the same as for ITER [9] except injection angle and frequency of the EC waves, which strongly depend on physics requirements and machine parameters, particularly the toroidal magnetic field. In a relatively hot and dense plasma, the power of the EC waves is absorbed in a single pass and its deposition is very localized, resulting in high power density. The spatial deposition is easily controlled through adjustment of the injection angles with respect to the toroidal magnetic field or the major radius or of the frequency. In the proposed FER supplementary scenario for current drive and heating, EC waves are considered for assist to plasma formation and controls of local electron temperature profile and of burn through a strong local electron heating.

The frequency of 140 GHz, corresponding to the cyclotron resonance frequency near the plasma center, appears appropriate for all these functions. It would be also suitable to choose 140 GHz of the frequency from technological point of view on RF source development. The EC waves are launched from the lower magnetic field side with a

fundamental quasi-ordinary mode. The injection angle is nearly perpendicular to the toroidal magnetic field. A poloidal scan of the microwave beam employed for FER allows control of the spatial deposition in the vertical plane.

Overall system design including transmission line, antenna, power supply and cooling system is described in Sec.2. The total system efficiency is also discussed in Sec. 2. In Sec.3, design and analysis on specific components, such as launching system, RF windows and neutron shield are presented. Conclusions, future prospects and R&D needs are presented in Sec. 4.

2. SYSTEM DESIGN

2.1 Outline of EC Wave System for FER

25 gyrotrons at 140 GHz, 1 MW/unit, CW are installed in a EC source room (see Fig.2-1) to guarantee the injection power of 20 MW in the plasma. It is considered that 5 MW of RF power is lost in a transmission line. Each RF source is fed by a dedicated 80-100 kV/DC, 3~5 MW(depending on gyrotron efficiency) power supply unit driven by a high frequency DC-DC converter. The RF power is very likely converted in the gyrotron from a cavity mode (whispering gallery mode) to a Gaussian-like beam by an optimized quasi-optical converter. By using a matching device, the output beam of the gyrotron efficiently couples to HE_{11} mode in a circular corrugated waveguide foreseen for low loss transmission to the tokamak. Special switches are used to improve the availability of the system, connecting different waveguides. Cryogenically cooled, sapphire window are employed to insulate the transmission line from the tokamak radioactive dust and tritium. Between the window and antenna, five bends for each channel are inserted to improve neutron and gamma screening of the ceramics of the window and to provide optimized geometry of the launching waveguides as shown in Fig.2-2 (a) and (b). In this design the twnty-five beams are transmitted into the launching system consisting of four reflectors. A second mirror is rotatable for scanning the beam. The last mirror produces desired beam characteristics at the plasma. The design of the launching system and the transmission line components has been conceived to allow integration of the EC system in the machine and possibility of remote maintenance.

The efficiency of the EC system is estimated to range between 25 % and 40 %. With 25 % efficiency and 20 MW of the injection power the requested electrical power is 79 MW and resultant 59 MW is dissipated in heat production. A cooling system capable of removing the heat is needed.

2.2 Gyrotron and Transmission Line

The EC power source for FER is 25 gyrotrons at 140 GHz and CW. Output power of a gyrotron is 1 MW, resulting in total power generation of 25 MW. The specification of the gyrotron required is listed in the following table.

Frequency	: 140 GHz
Output Power	: 1 MW
Output Mode	: Gaussian-like beam mode

Pulse Duration	: CW (2 weeks)
Efficiency	: 35 %
	> 50 % (using a collector potential depression)

The output mode of the gyrotron is a Gaussian-like beam, which is produced from the cavity mode by a built-in mode converter. The efficiency including the mode converter is expected to exceed 50 % by using a collector potential depression system.

The transmission line combines the advantages of HE_{11} circular waveguides and TEM_{00} quasi-optical waveguides, providing low transmission losses and tritium containment. The output beam of the gyrotron efficiently couples to the HE_{11} mode of a corrugated waveguide by appropriate quasi-optics matching devices. RF power is transmitted from RF source room to the launching system installed in a torus hall with a bundle of 25 corrugated waveguides. A largely oversized waveguide with 88.9 mm in inner diameter is used. Miter bends are used in a layout of the transmission line. The average length of the transmission line is about 150 m including the launching system. The transmission line is evacuated to increase power capability and to allow decontamination.

A cryogenically cooled RF window is placed at entrance of the launching system to avoid spread of tritium and radioactive dust coming from the tokamak. A part of the transmission line near the window assembly has to be kept in a good level in vacuum to avoid any possibility of frost of gases (H_2O, O_2, N_2 etc.) on the ceramic surface of the window.

Optics of the launching system is composed of four mirrors. The poloidal scanning of the RF beam is possible in time with rotating the third mirror. The scanning range of the beam is z=0~2500 mm in the vertical plane at the plasma center. A quantitative analysis is described in Sec. 3.1. This would be useful for the control of the electron temperature and associated current profiles to improve the plasma performance.

The transmission line efficiency including the launching system is given by

Coupling between the Gyrotron Output and and the HE_{11} Waveguide	: 94 %
Corrugated Waveguide	: 96 %
14 Miter Bends	: 93 %
Window	: 99.5 %
Coupling from HE_{11} to Gaussian Beam	: 98 %
Launching System	: 98 %
Total Efficiency	: 80 %

2.3 Power Supply System

For the design of the main power supply system, CW triodes gyrotron for necessary high stability requirements are considered. Power supply unit for each gyrotron is composed of a series regulator having the following characteristic: 3~5 MW power (depending on gyrotron efficiency) ; DC voltage 80~100 kV (regulation less than +- 0.2 %); turn on time about 100 microsecond; turn off time about 15 microsecond (for tube protection) ; current 40~50 A. Optimization of the power supply characteristics will be necessary knowing final parameters of a gyrotron. The power supply for short pulse operation can easily satisfy the requirement of fast turn off by means of application of a crowbar circuit in DC high voltage line. However, it would be hard to employ the crowbar circuit in CW operation power supply system because rectifier and transformer winding coil must not only satisfy their cooling requirement but also withstand the magnetic force generated by excessive current when the crowbar is fired .

A new kind of power supply, without the crowbar circuit and where fast turn-on and off as well as the voltage regulation are accomplished by a high frequency DC-DC converter, is employed to drive the CW gyrotron. Figure 2-3 shows the schematic diagram of the power supply system. The system consists of a low voltage AC-DC converter, high frequency inverters, step-up transformers and high voltage DC converters. The latter three components work as a DC-DC converter. Each high DC-DC converter is connected in series. The DC-DC converter is operated with the frequencies of ~100 Hz up to several kHz which allow to decrease core size of the step-up transformer and then to reduce its leakage inductance. In order to decrease energy stored in high voltage line, which makes a fast turn-off function worse, the DC-DC converter should be located close to gyrotron as shown in Fig.2-4. Although a capacitor bank for a filter is not employed, a stray capacity between high voltage line and earth has to be taken account for. One of the DC-DC converters operates as an active filter. [10] The size of the DC-DC converter system is estimated as 1500 mm (W) x 3000 mm (D) x 3200 mm (H) per a gyrotron. The size of the room for the power supply will be 30 m (W) x 14 m (D) x 12 m (H). This system will be capable of the efficiency superior to 95 %, which leads to reduction of heat production, resulting in relaxation of cooling requirements.

2.4 System Efficiency and Cooling System

The reference efficiencies in power are listed in the following table.

	Efficiency	
	min. expected	desirable
Power Supply	0.9	0.95
RF Source (Gyrotron)	0.35	0.5
Transmission Line	0.8	0.85
Total	0.252	0.404

The overall efficiency of the EC system is expected to be about 25 %. The design of neutron shield for the transmission line would require several additional bends which would deteriorate the efficiency of the transmission line. Possible technological improvements within FER/ITER time-scale could lead to an increase of the overall system efficiency up to 40 %.

With 25 % of total system efficiency, power flow for 20 MW RF system is shown as follows.

Requested Electrical Power (AC)	79.4 MW
Gyrotron Input Power (DC)	71.4 MW
Transmission Input Power (RF)	25 MW
RF Power Launched to Plasma	20 MW

The total power loss is 59.4 MW which is dissipated in heat production. Cooling system capable of removing that heat is needed.

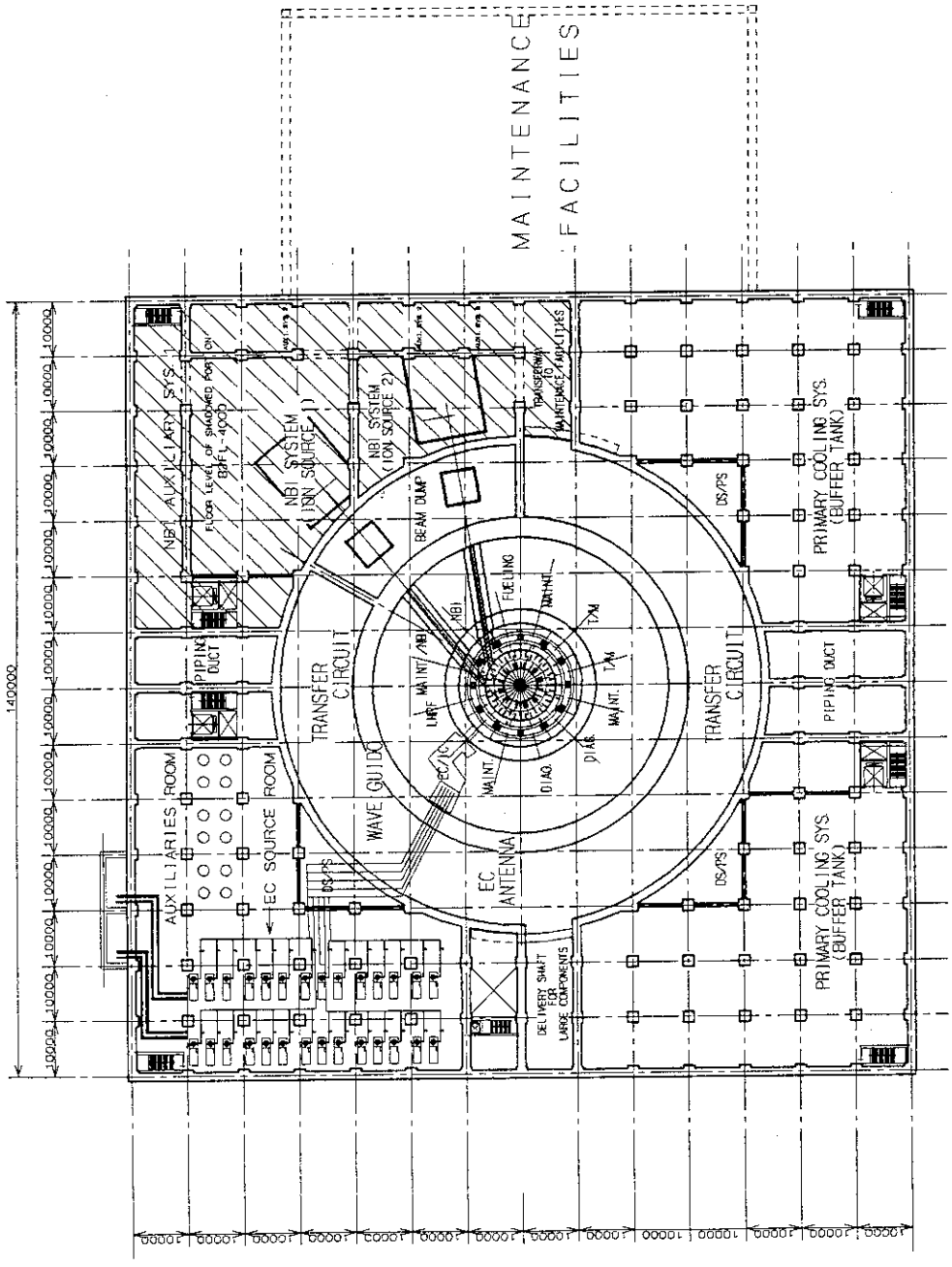

BLOCK PLAN

Fig.2-1 Integration of the EC system in the tokamak building: basic requirement schematic plane view

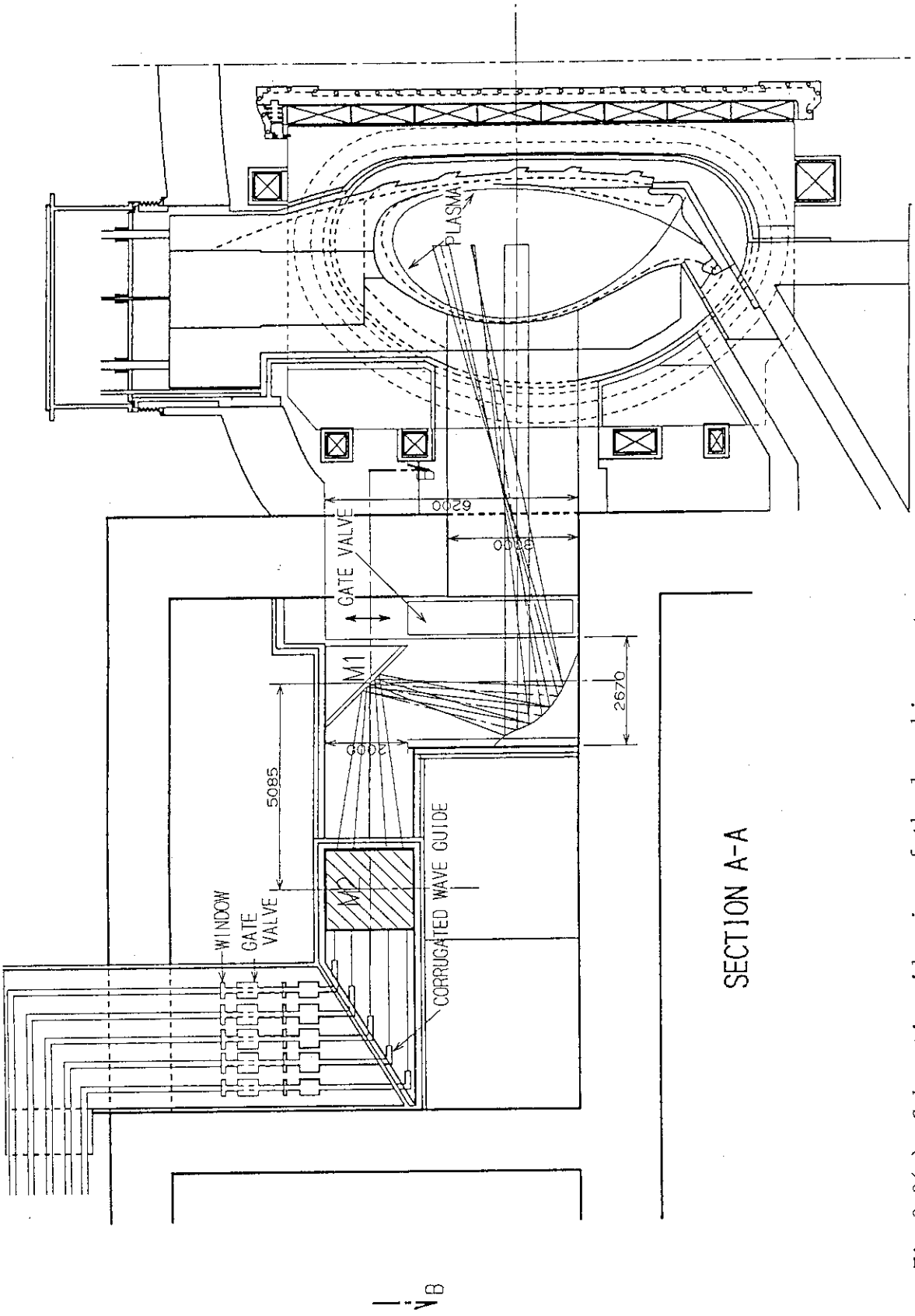

Fig.2-2(a) Schematic side view of the launching system

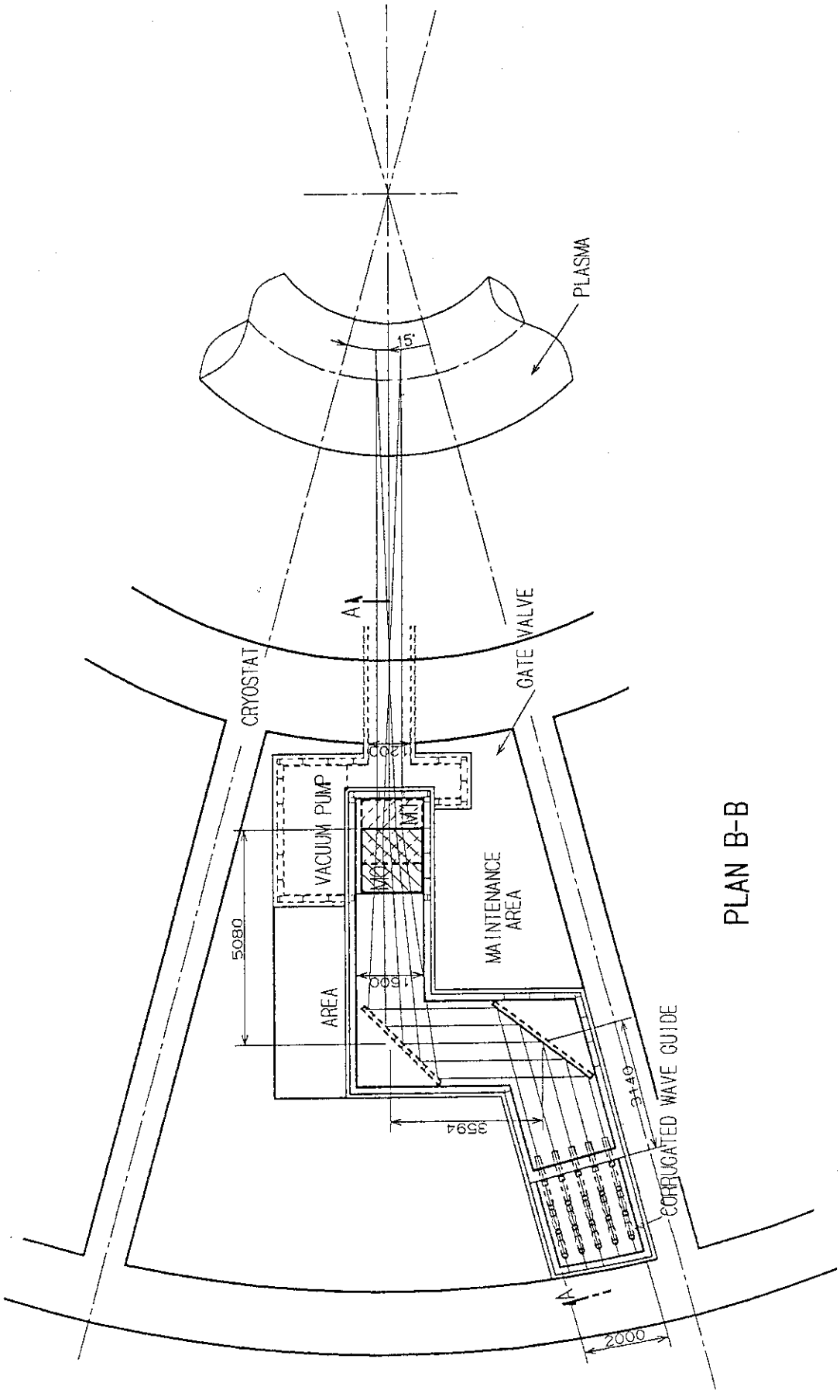

Fig.2-2(b) Schematic top view of the launching system

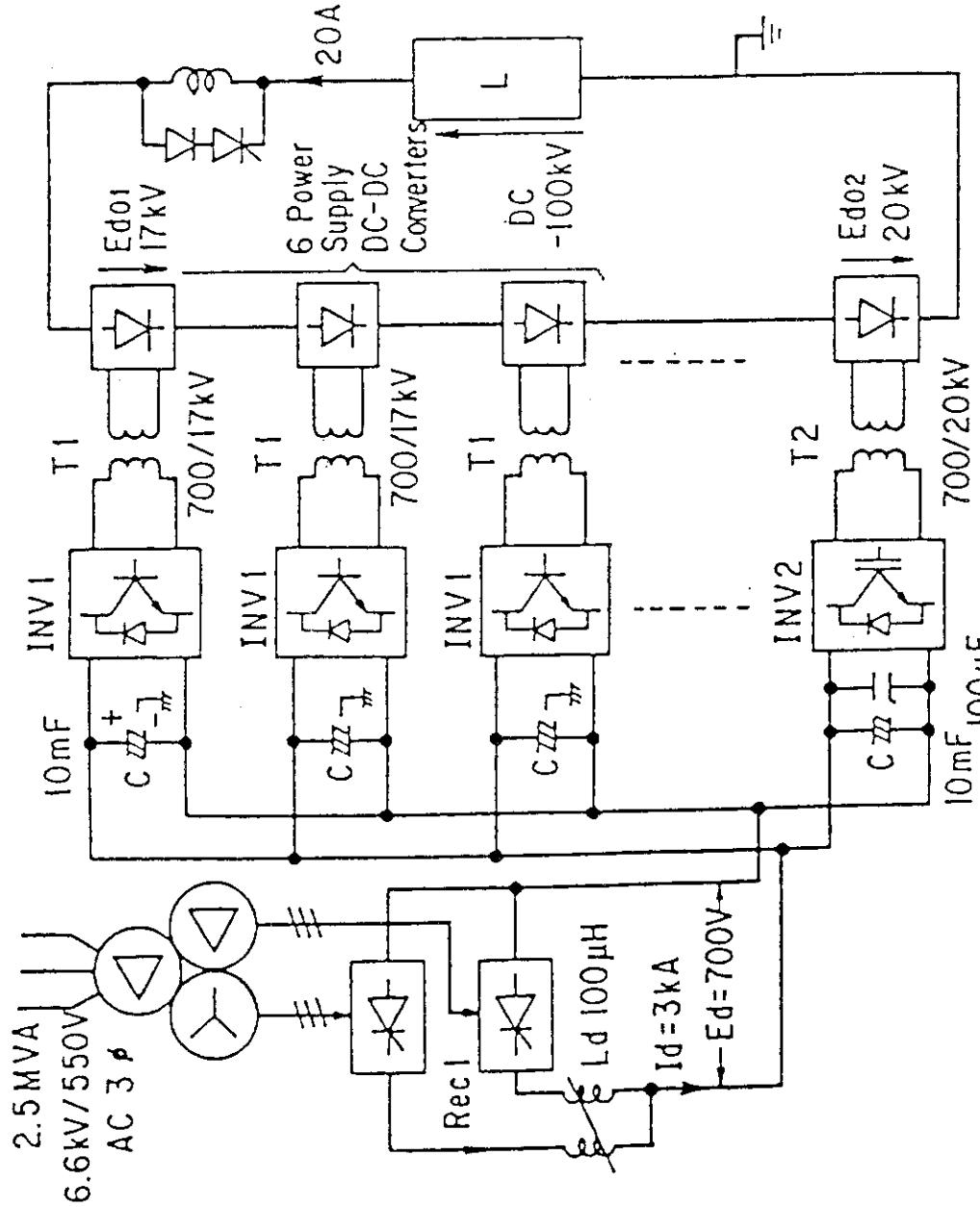

Fig.2-3 Schematic diagram of a 2 MW power supply system

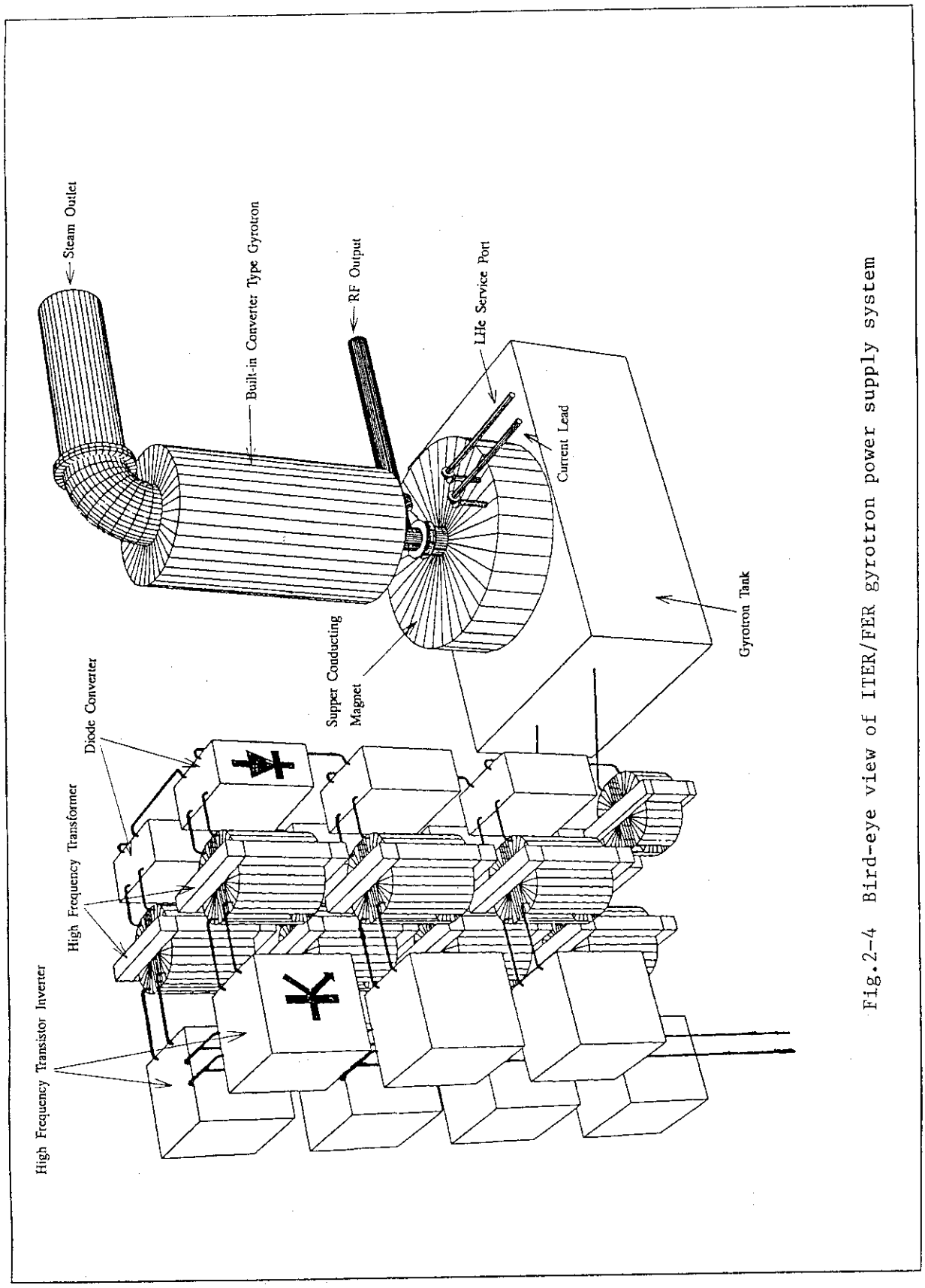

Fig.2-4 Bird-eye view of ITER/FER gyrotron power supply system

3. SUBSYSTEM DESIGN AND ANALYSIS

3.1 Launching System

The main objectives of EC system for FER are plasma formation in the start-up phase and suppression of instabilities through a control of the electron temperature and current profiles. To satisfy these physics requirements for beam size, divergence and scanning angle, the launching system has been optimized from the optical point of view. When waves are injected nearly perpendicularly to the toroidal magnetic field and the beam line is scanned in the poloidal direction, the spatial position of RF power deposition in a plasma changes in the vertical plane, resulting in modification of the temperature profile. An appropriate profile would be expected to make the plasma stable. When the beam line is scanned in the toroidal direction, that is, injection angle with respect to toroidal magnetic field changes, the position of the deposition can be changed through effect of Doppler-shift in the resonant interaction of the waves with electrons. In this case, a local current drive would be expected and then stabilize the plasma instabilities effectively.

3.1.1 Launching system for FER

For EC system of FER, the poloidal scan of the beam is a first candidate because of simplicity of the system and of compatibility with IC system. RF power of 20 MW is injected into the plasma nearly perpendicularly to the toroidal magnetic field in the 0-mode through a horizontal port with the size of 1200 x 3000 mm^2. The twenty-five beams are radiated from an open-ended (HE_{11} carrying) waveguide array with a divergence of the individual beams. The inner diameter of the waveguide is 88.9 mm and the waveguides are bundled in 5 x 5 array. The spacing between waveguides at the exit is 400 mm. Tritium is sealed by a double sealed ceramic window. The window is cryogenically cooled to improve the power capability. This is one of the possible methods to realize 1 MW, CW, RF window at the high frequency. The launching system is evacuated in high vacuum and the beams are bended by one miter bend and four mirrors. In Fig.3-1, composition of a mirror array and the beam lines are illustrated. The positions of each items are listed in Table 3-1 and curvature of the mirrors are cited in Table 3-2. The mirror M2 and M4 are focusing mirror and other two mirrors have a flat surface(see Fig.3-1). The mirror M3 is rotatable for scanning the beam in the poloidal direction. The mirror M4 has an elliptical surface whose focusing points are R and S on the M2 mirror. The point R denotes the crossing point between the line A and line B, where A refers to the line between the center of the output port and the upper point on the mirror M1 and B the line between upper side of output

port and the lower point on the mirror M1 (see Fig.3-1). Then the following relation is obtained;

$$\frac{1}{f_1}=\frac{1}{RM1}+\frac{1}{M1M2}=\frac{1}{PM1}+\frac{1}{QM1},$$

where the point Q is the conversion point of beamlets by the M3 mirror. (QM2 + M2M3= 6.8 m). The beam line parameters are shown in Table 3-3. The three-dimensional pictures and the power distribution of the total beam at two different points are illustrated in Figs.3-2 and 3-3, respectively.

3.1.2 Launching system for ITER

In ITER , the injection of 20 MW, CW at 120 GHz into the plasma for local current profile control near the q=2 surface has been considered for the reference magnetic field of the machine (4.85 T). The launching system, allowing an oblique RF radiation and plasma scanning in an horizontal plane, is installed in an horizontal port and uses half of the port area. In the present design the injection is in a quasi-ordinary mode from the outboard side close to the equatorial plane at about 20° with respect to the major radius direction. The specification of the beam line for the launching system of ITER is as follows.

Frequency	:	120 GHz
Number of Beam	:	4 x 7
Dia. of waveguide	:	88.9 mm
Injection Angle	:	15°~25° (at the port exit in the horizontal plane)
Mirrors	:	four mirrors
Divergence of injection	:	< 1°

In Figs. 3-4 (a)-(c), the result of the optical optimization for the launching system are illustrated. Twenty-eight beams are radiated by an open-ended corrugated waveguide array with the natural divergence of the individual beams. The beamlets are collected by a mirror M1 which combines the beamlets in a way to have on the rotatable (flat) mirror M2 the same image as desired at the rotating point close to the plasma. The narrowest diameter (waist) of the multi-beam is between the rotatable mirror and the third mirror M3. The duct between the two boxes allows a relatively small hole in the antenna shielding between the two main boxes to reduce solid angles for neutron propagation. Its geometrical-optical image is such that the beamlet crosses in a plane containing the axis of the torus, therefore, each beamlet dose not contribute to the total horizontal beam divergence (see APPENDIX). Namely, the multiple beam divergence is equal to the divergence of a single beamlet. The requirements for the vertical divergence are less

stringent because the current drive efficiency and localization of the current drive are not sensitive to the beam divergence perpendicular to the magnetic field line. The third reflector with flat and wide surface is needed to fold the beam in the proper way on the last mirror M4. The last reflector is an ellipsoidal mirror which produces the desired beam characteristics without aberrations during the sweeping. These two last mirrors are fixed and have large surface in order to intercept the scanning beam. The size of the beam bundle at the plasma edge is of about 40 cm in the horizontal and 50 cm in the vertical direction, but the effective beams size is about 10 cm as shown in Fig.3-5. The effective horizontal and vertical divergences are about 1° and 3° respectively (see Fig. 3-6).

3.2 RF Window

Reliable RF vacuum window is supposed to be placed at the gyrotron exit and the tokamak entrance. The window design, the position of the window assembly in the launching system, and the material behavior under and after irradiation are inter-related closely each others. In this section, analysis of the cryogenically cooled window is described from the thermo-mechanical point of view. At low temperature, many parameters of the material used that enter in determining the window stress are much improved. As a result, thermal stress is no longer the limiting mechanism at cryogenic temperature.

A double disk window, as shown in Fig.3-7, in which a cryogenically coolant gaseous helium is flowed between the two disks to remove a heat is considered here. The specification for conceptual design of the window is as follows;

Material	Sapphire (Single crystal aluminum oxide)
Structure	Double disks
Cooling	Surface cooling by a cryogenical coolant gaseous helium
Frequency	110 GHz
Transmitted Power	1 MW
RF mode	HE_{11}
Dia. of Waveguide	60.325 mm
Pressure in Waveguide	< 1.33 Pa

We have calculated stresses of the disk resulting from temperature distribution, using the heat conduction equation. In the calculation, the following parameters were used.

Loss Tangent of Dielectric	: $\tan\delta = 5.58 \times 10^{-11} f^{0.717} T^{1.96}$ 11) with f of frequency in GHz and T of temperature in degrees Kelvin
Heat Transfer Coef.	: H= 0.174 (Wcm^{-2} deg^{-1})
Density of Sapphire	: 3.97 g cm^{-3}
Young's Modulus	: 480 GPa
Poisson's ratio	: 0.29
Specific Heat	: 0.76 J g^{-1} deg^{-1}
Thermal conductivity	: 5 W cm^{-1} deg^{-1}
Coef. of liner expansion	: 0.1 x 10^{-6} deg^{-1}
Relative dielectric Const.	: 9.4
Thickness of disk	: 1.33 mm

Dielectric heating of the disk appears to the most crucial aspect of the cryogenic window. Figure 3-8 shows the radial profile heat deposition due to dielectric heating at the temperature of 77 K. The heat density is the maximum at the center and its e-folding length is 17 mm. The radial profiles of increase in the temperature on the disk and resulting thermal stresses are shown in Fig.3-9. The solid and broken lines in the lower figure denote the tangential and radial stresses, respectively, and the positive and negative values correspond to the tension and compression stresses, respectively. The results calculated are obtained in the steady state at the initial temperature of 77 K. It is seen that the maximum tension and compression stresses are 1.25 and 0.6 MPa, respectively. These value are very enough less than the maximum allowable values, namely 2300 MPa in tension and 3000 MPa in compression. This result indicates that the thermal stresses are negligible small. Also, the results at the initial temperature of 40 ° K are shown in Fig.3-10. The lower temperature operation leads to decrease in the incremental temperature of the disk and then lessens the thermal stresses further.

3.3 Radiation Shield for RF Window

At present it is quite hard to estimate neutron radiation effects on the window assembly because of a few database on them. According to the ITER meeting [12], dose limit of the window ceramic seems to about 10^{18} n/cm^2. However, 10^{16} n/cm^2 should be probably recommended to avoid significant degradation of the loss tangent and the thermal conductivity.

In ITER technology phase, the average neutron fluence is 1~3 MW/m^2 and the machine availability is 10 % . As a result , 6 x 10^{25} na/m^2 neutron are generated at the

first wall. If the window assembly is replaced in every year, neutron flux at the window should be attenuated by a factor of 5~6 orders from radiation at the entrance of the machine port. Figure 3-11 shows the distribution of nuetron and gamma ray fluxes along NBI duct axis. [13] It is inferred that from Fig. 3-11 that the distance between the plasma and the final mirror makes the neutron flux decreased by about two order. A 90 degree bend is estimated roughly to yield 10 dB attention of neutron. Figure 3-12 shows neutron flux distribution along the center line of the RF duct.[14] To shield the windows by 5~6 orders from neutron radiation of the plasma, the final mirror would be required to be installed 7~8 m far from the first wall. Figure 3-13 shows the neutron shield structure of the launching assembly for FER.

Table 3-1 Position of the item on the beam line of the launching system

	CENTER COORDINATES		
LINE-ITEM	X-COORD (m)	Y-COORD (m)	Z-COORD (m)
0	0.0	-4.4	3.6
1	3.0	-3.6	3.6
2	3.0	0.0	3.6
3	8.1	0.0	3.6
4	7.8	0.0	-0.7
5	10.0	0.0	-0.32
6	16.2	0.0	0.75
7	18.6	0.0	1.16

ITEM NO.	
0	waveguide cut
1	flat mirror
2	curved mirror
3	rotatable flat mirror
4	curved mirror
5	port entrance
6	port exit
7	plasma center

Table 3-2 Curvature of mirrors of the launching system

RADII OF CURVATURE OF MIRRORS			
LINE-ITEM	P-ANGLE(DEGS.)	P-CURV. (m)	S-CURV. (m)
1	52.5	1.0E05	1.0E05
2	45.0	18.7	9.33
3	43.0	1.0E05	1.0E05
5	38.1	4.88	3.02

P-ANGLE : Reflection Angle

P-CURV. : Curvature of Mirror in the direction of P-angle

S-CURV. : Curvature of Mirror in the perpendicular direction of P-angle

Table 3-3 Beam line parameters of ECW system for FER

FER ECH BEAM LINE PARAMETERS (ROTATION ANGLE < +- 3.4 DEGS)				
ITEM-NO	P (m)	FH/FV (m)	H/V (m)	SH/SV (m)
0	0	1.0E05/1.0E05	1.69/1.69	2.93/2.93
1	3.1	1.0E05/1.0E05	3.14/1.99	7.79/7.79
2	6.7	3.6/3.6	3.3/2.23	15.9/15.9
3	11.8	1.0E05/1.0E05	0.759/1.04	5.50/5.50
4	16.1	1.92/ 1.92	0.86/ 2.78	6.53/6.53
5	18.3	1.0E05/1.0E05	0.821/2.11	4.30/4.30
6	24.6	1.0E05/1.0E05	0.805/3.22	10.5/10.5
7	27.1	1.0E05/1.0E05	1.33/5.1	14.9/14.9

P : beam propagation length

FH : focal length in horizontal plane

FV : focal length in vertical plane

H : size in horizontal plane

V : size in vertical plane

SV : horizontal spot size

SV : Vertical spot size

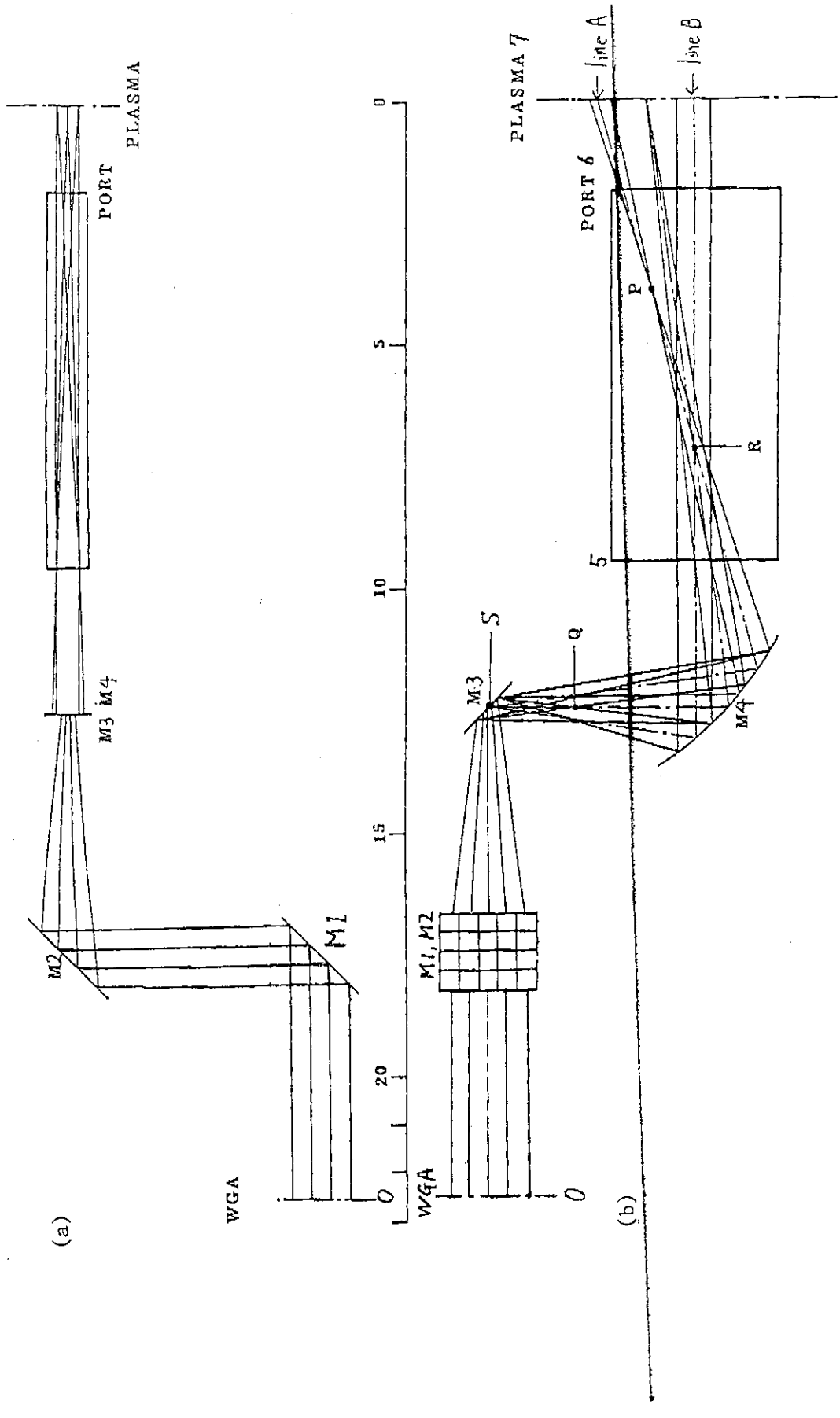

Fig.3-1 Conceptual configuration of beam line: (a) horizontal plane and (b) vertical plane

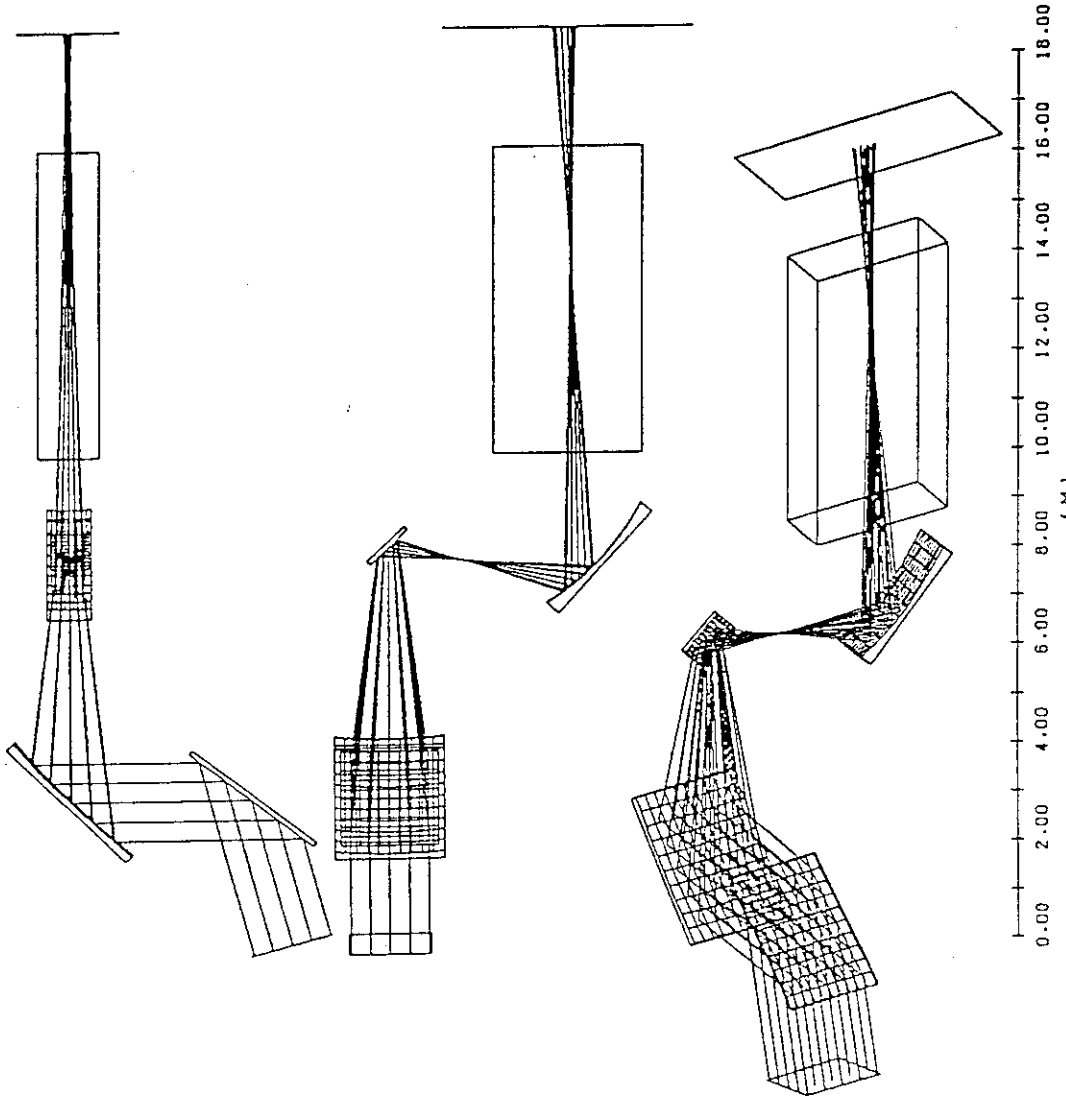

Fig.3-2(a) Three-dimensional pictures of beam lines for three typical positions of z=0 m

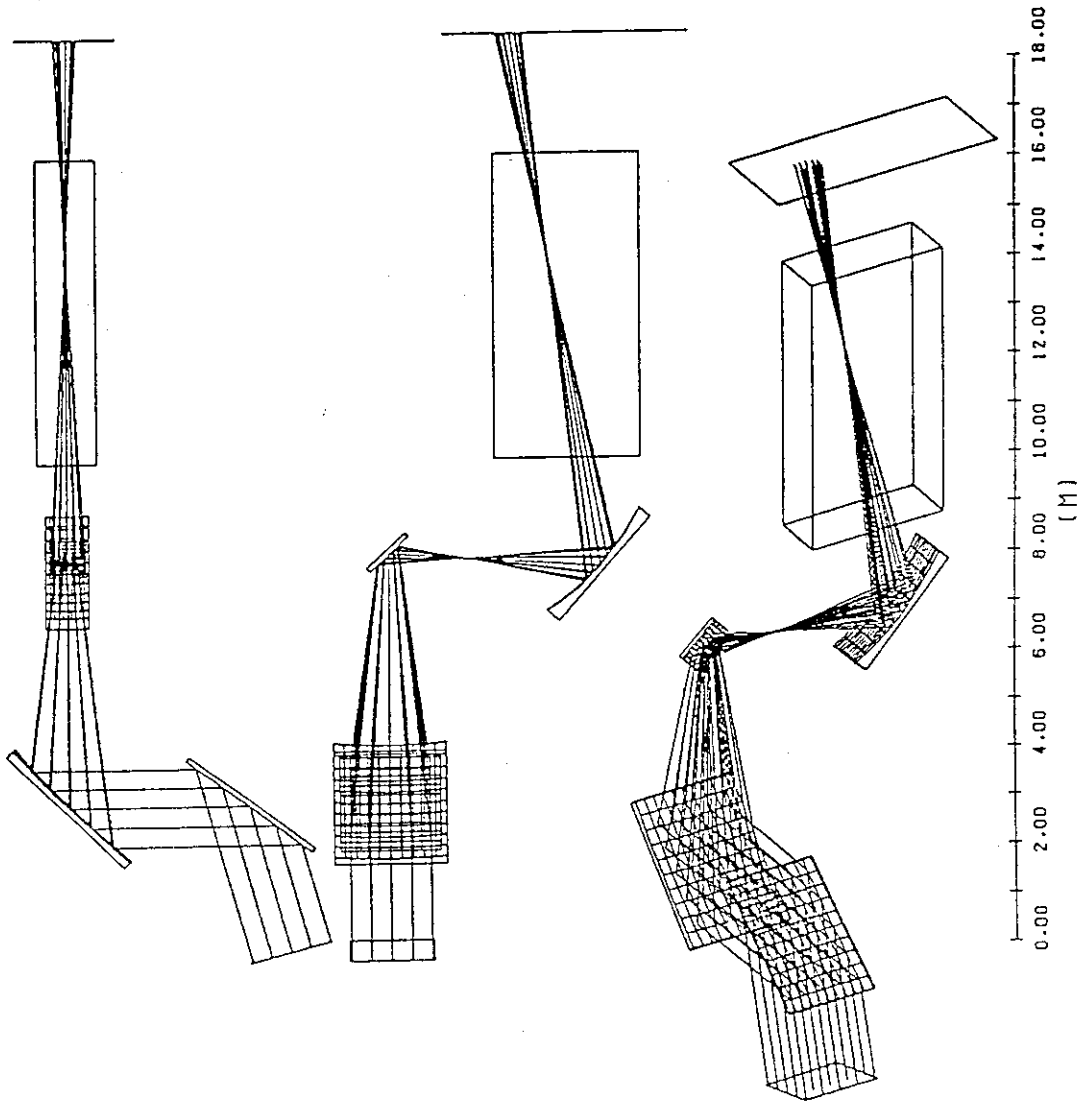

Fig.3-2(b) Three-dimensional pictures of beam lines for three typical positions of z=1 m

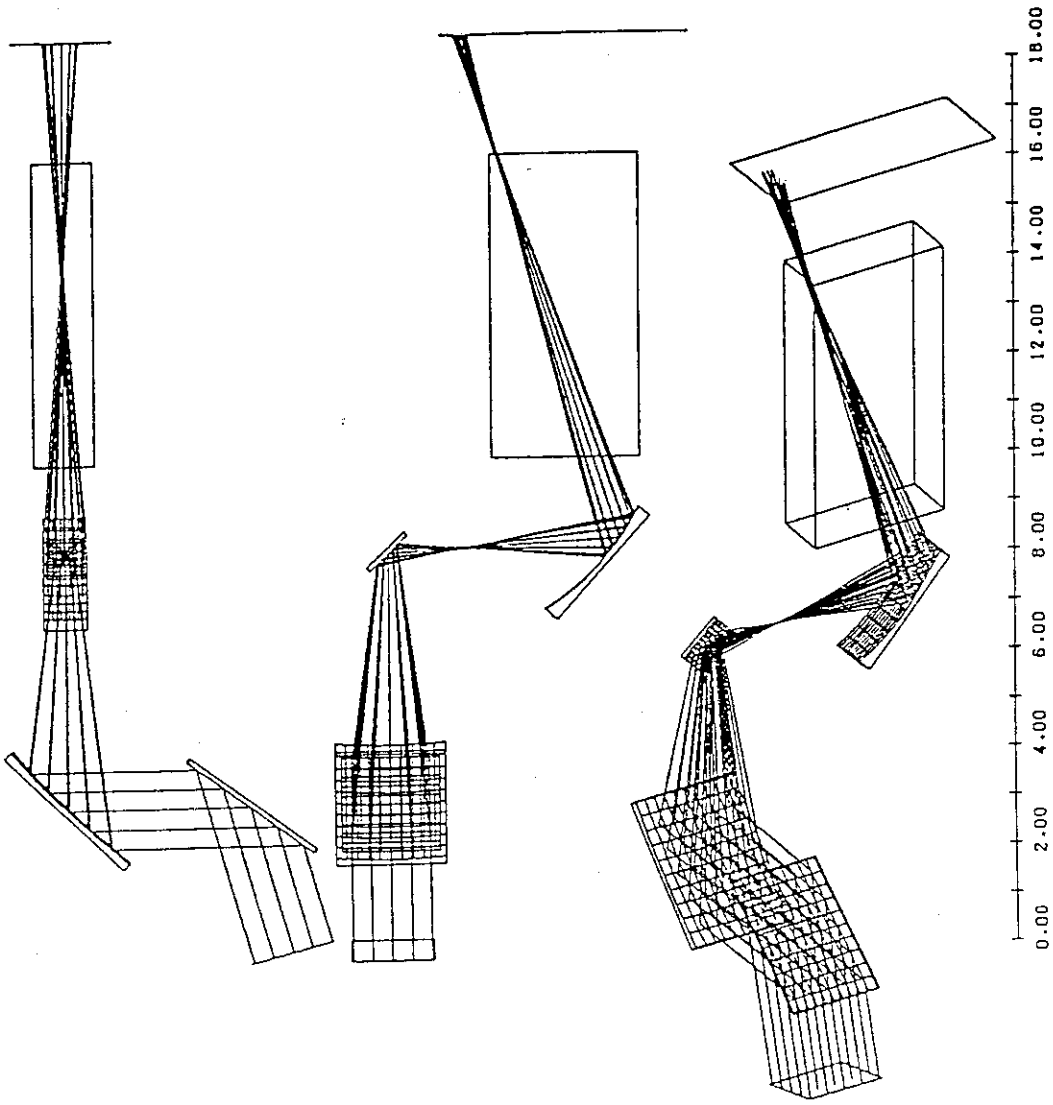

Fig.3-2(c) Three-dimensional pictures of beam lines for three typical positions of z=2 m

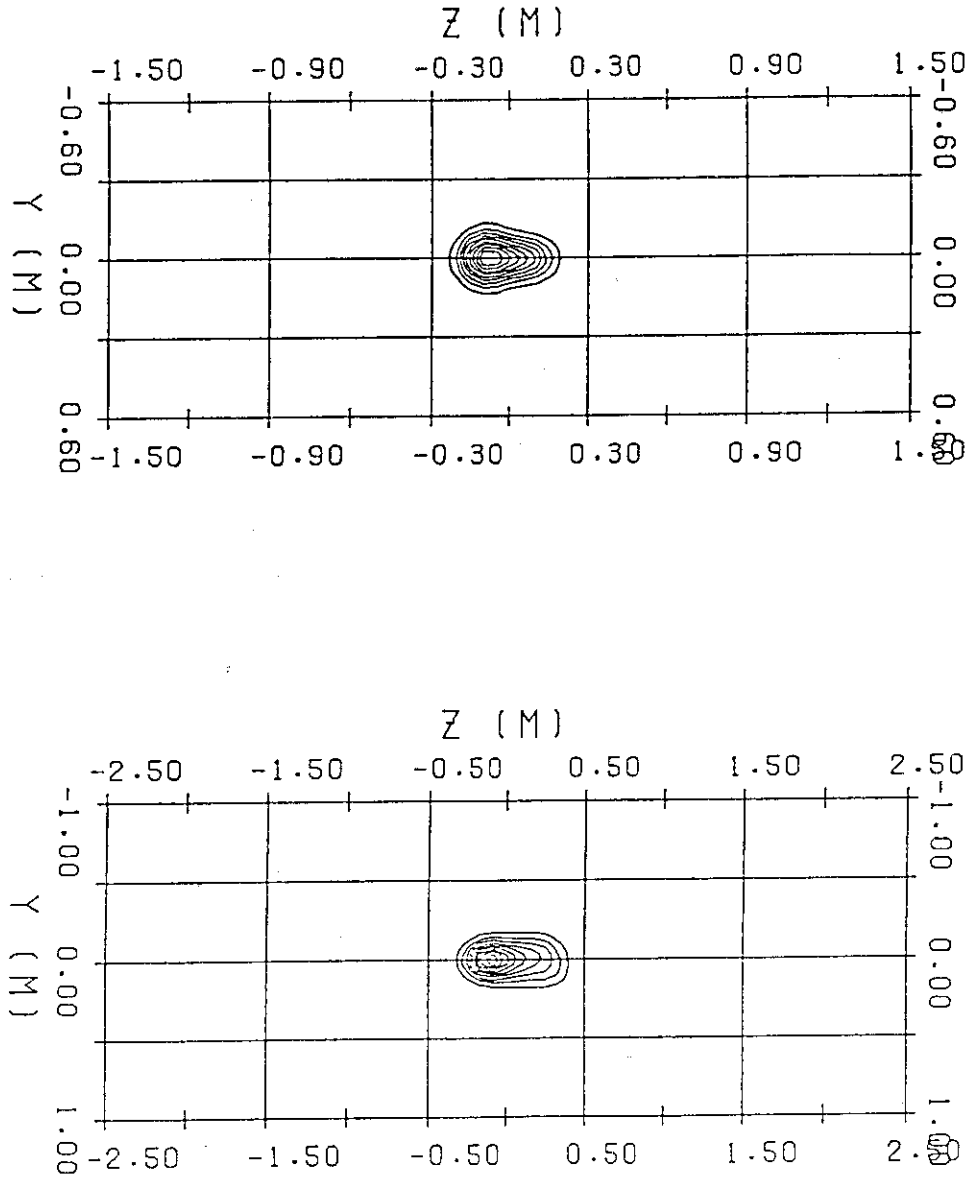

Fig.3-3(a) Shape of the radiated beams for the same as in Fig.3-2(a). The top and bottom show the power distribution at the port exit and the plasma center, respectively. The coordinate is the same as in Fig.3-1.

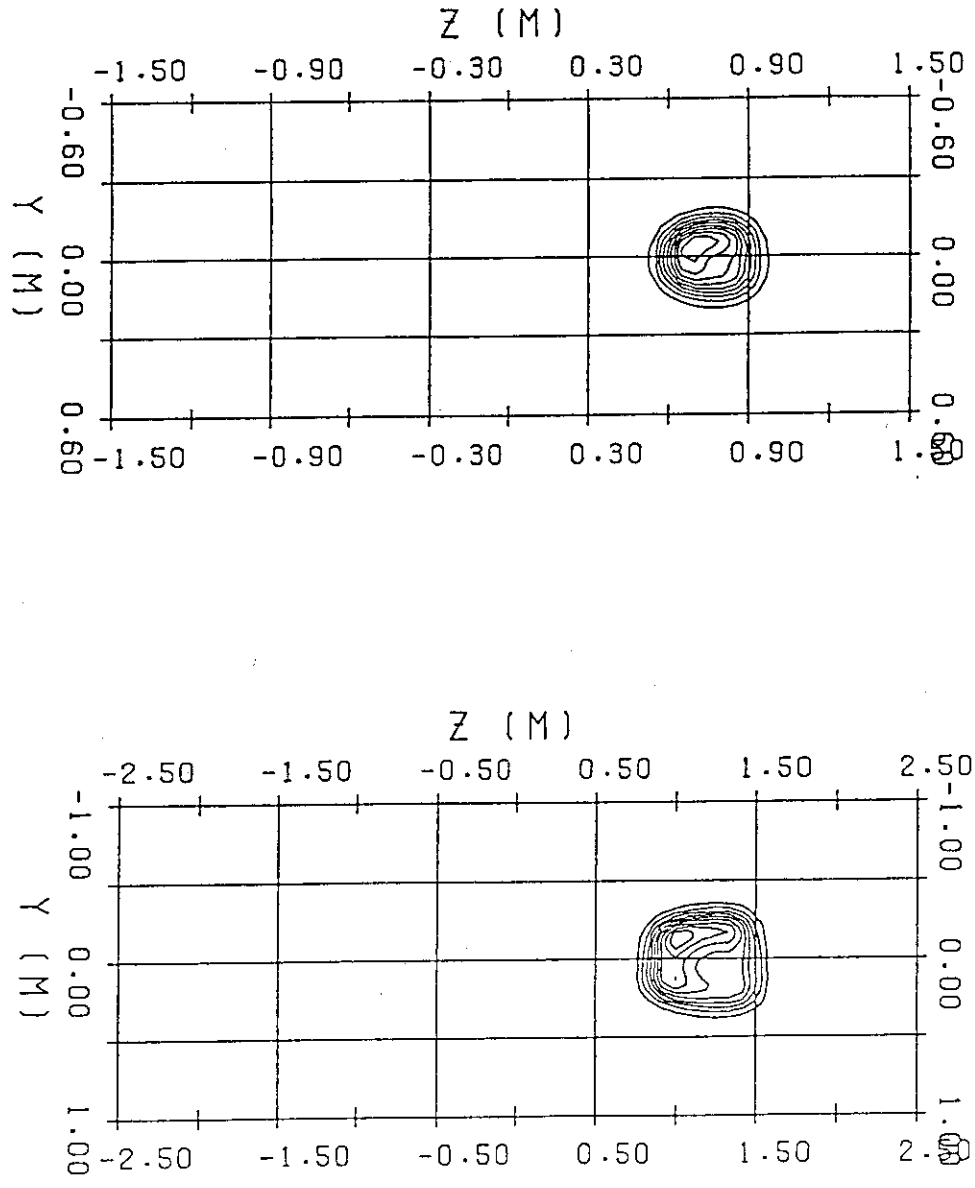

Fig.3-3(b) Shape of the radiated beams for the same as in Fig.3-2(b). The top and bottom show the power distribution at the port exit and the plasma center, respectively. The coordinate is the same as in Fig.3-1.

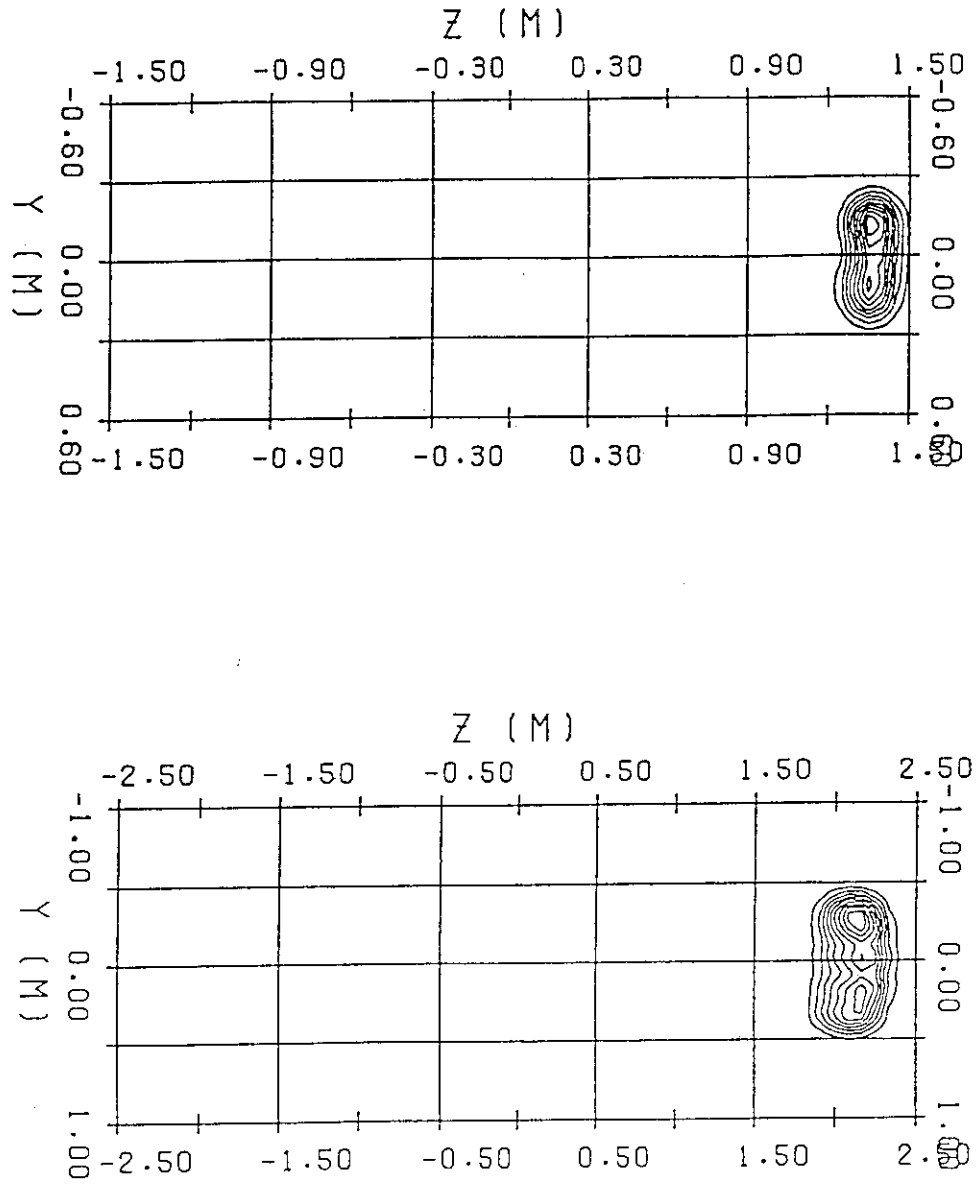

Fig.3-3(c) Shape of the radiated beams for the same as in Fig.3-2(c). The top and bottom show the power distribution at the port exit and the plasma center, respectively. The coordinate is the same as in Fig.3-1.

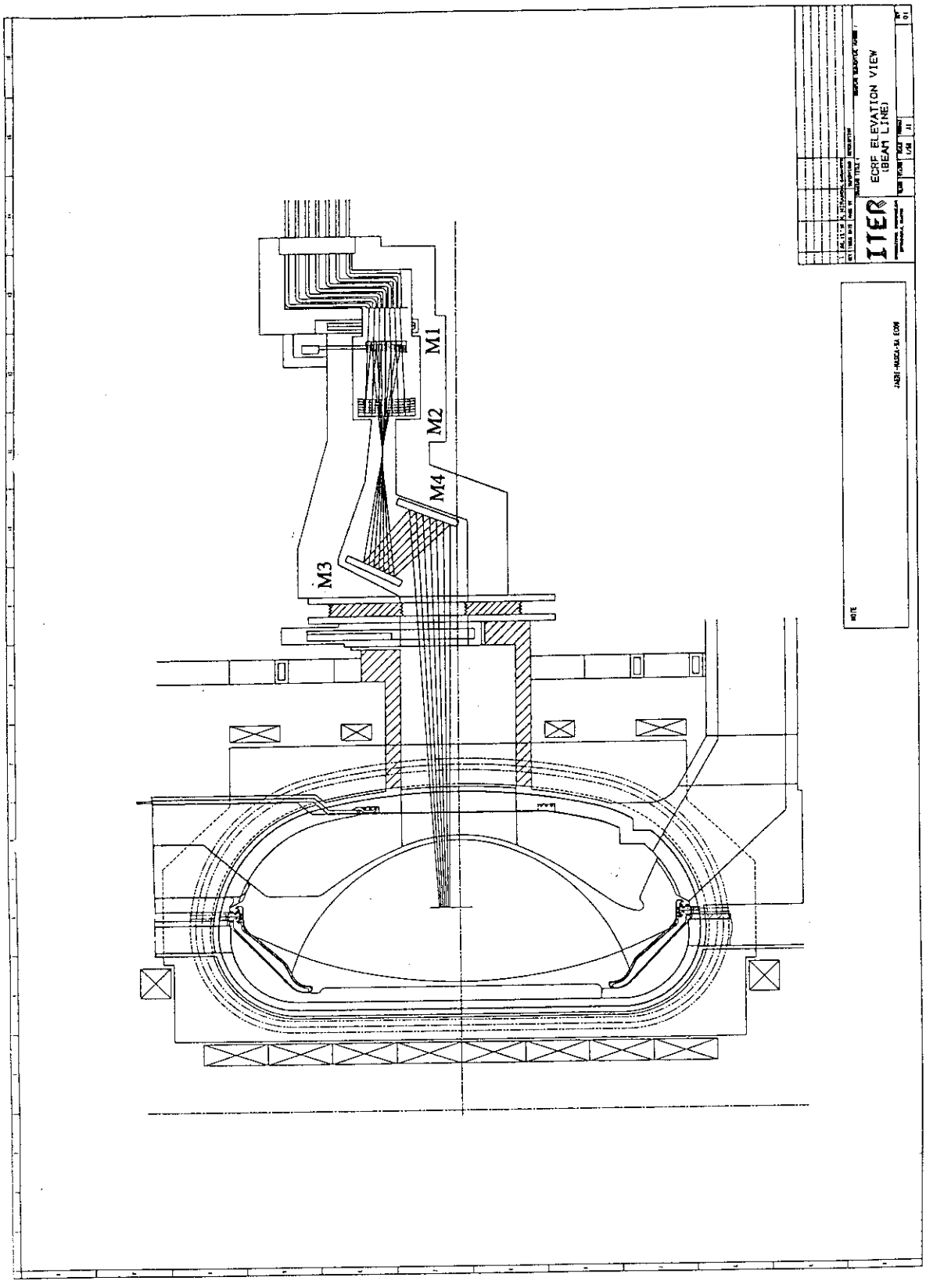

Fig.3-4(a) Two-dimensional drawing of the launching system for ITER ECW system, side view

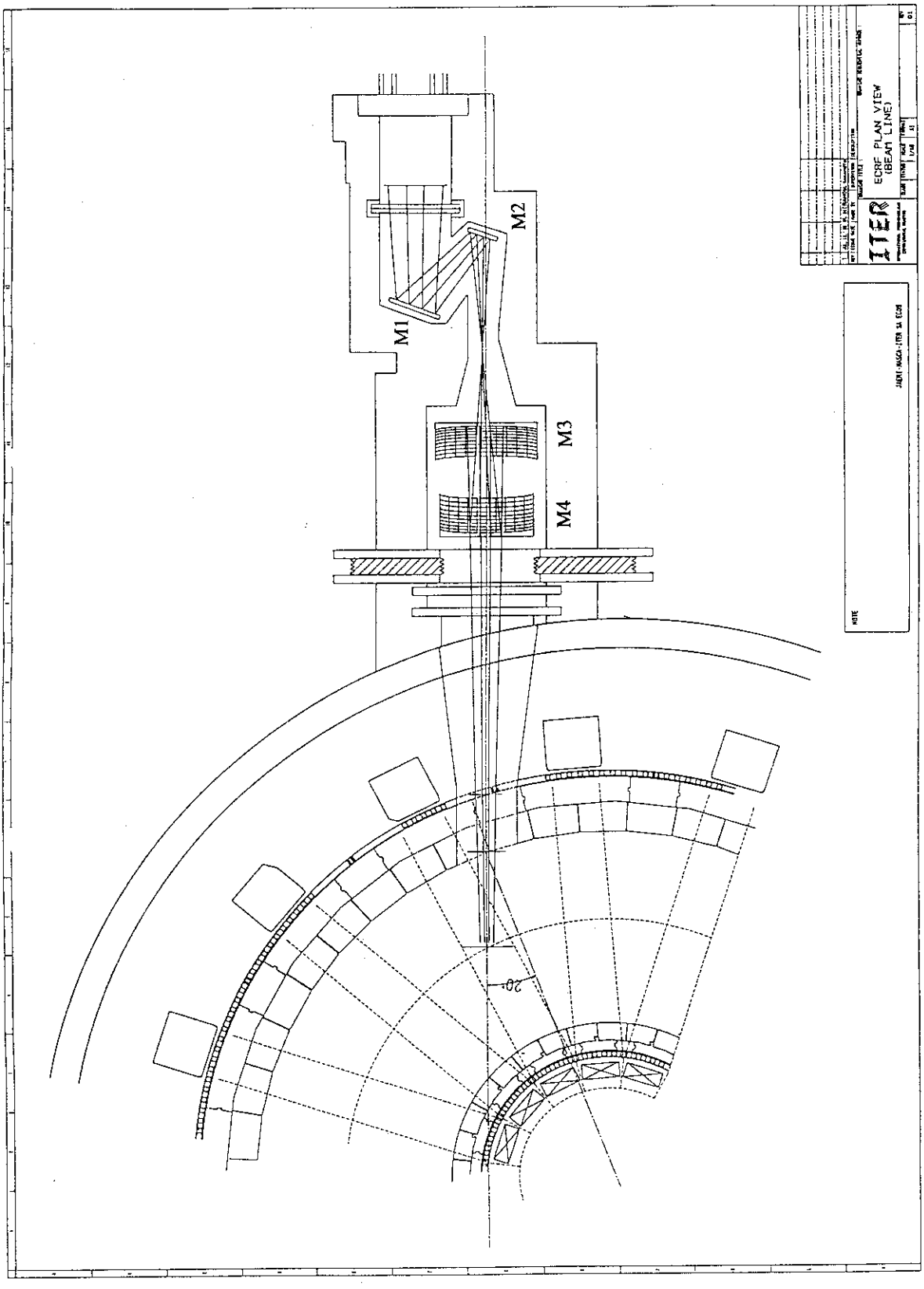

Fig.3-4(b) Two-dimensional drawing of the launching system for ITER ECW system, top view with the injection angle of 20°

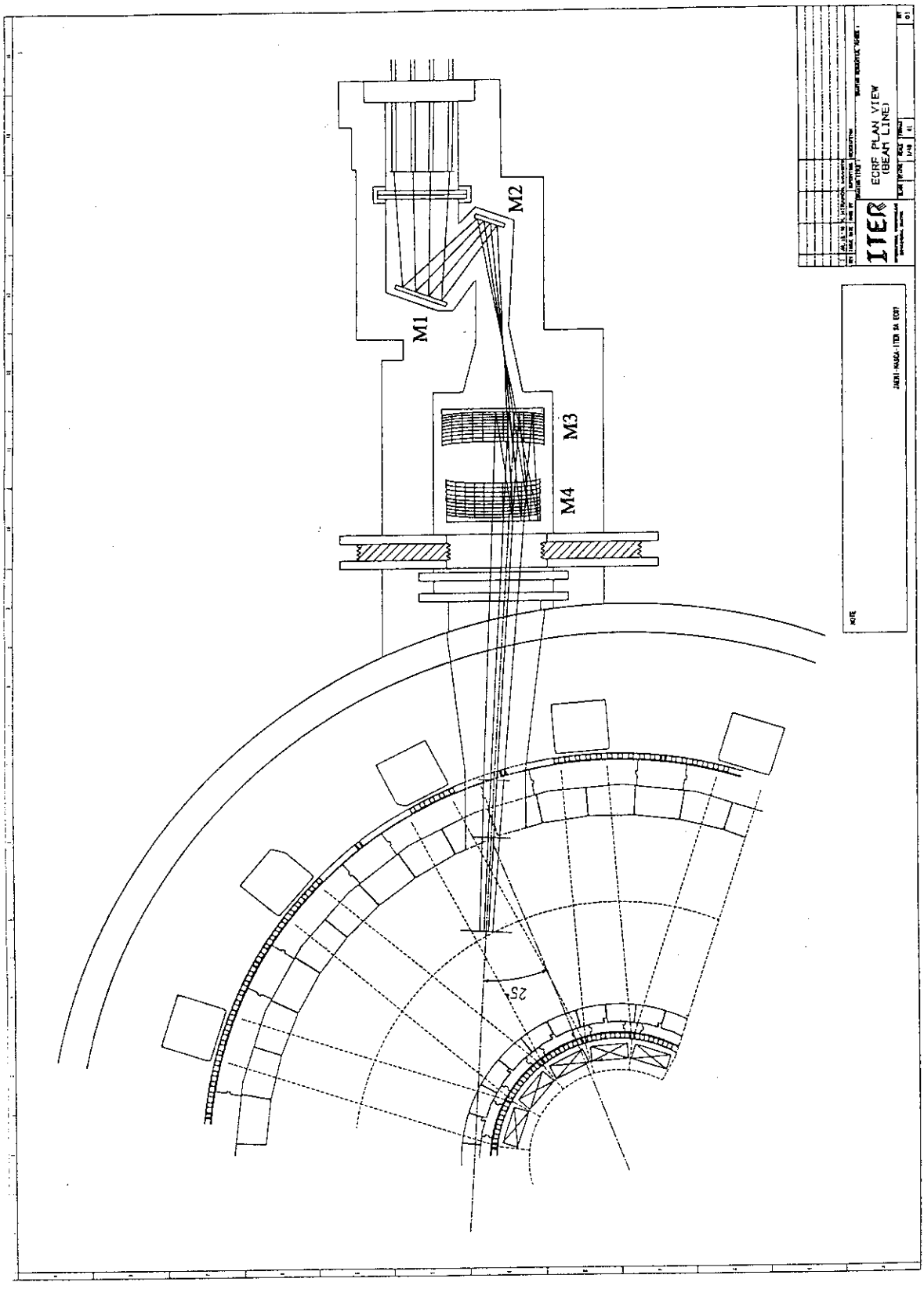

Fig.3-4(c) Two-dimensional drawing of the launching system for ITER ECW system, top view with the injection angle of 25°

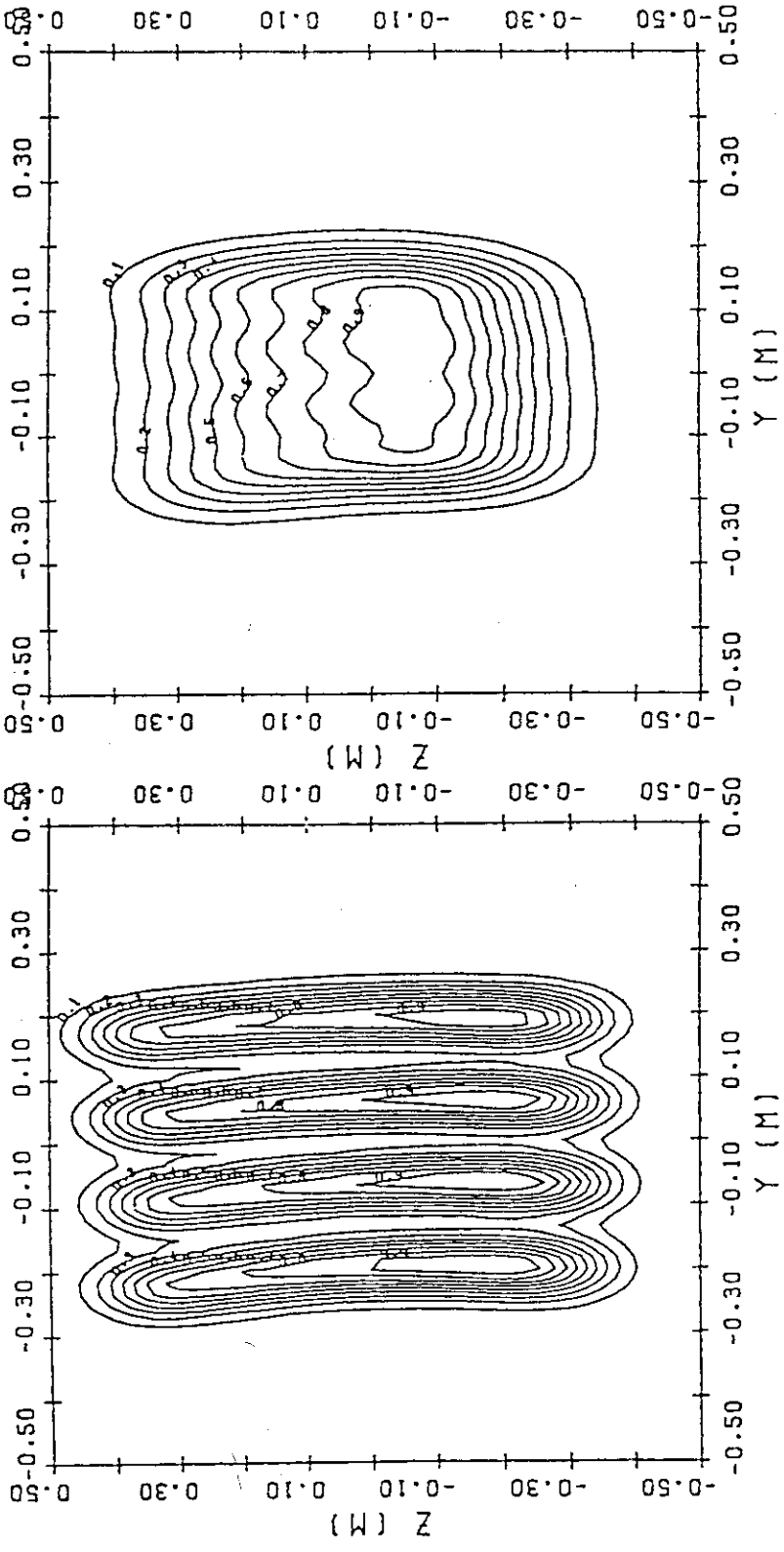

Fig.3-5 Shape of the radiated beam for the injection angle of 20° at the narrowest point of the duct (left) and at the q=2 magnetic surface (right)

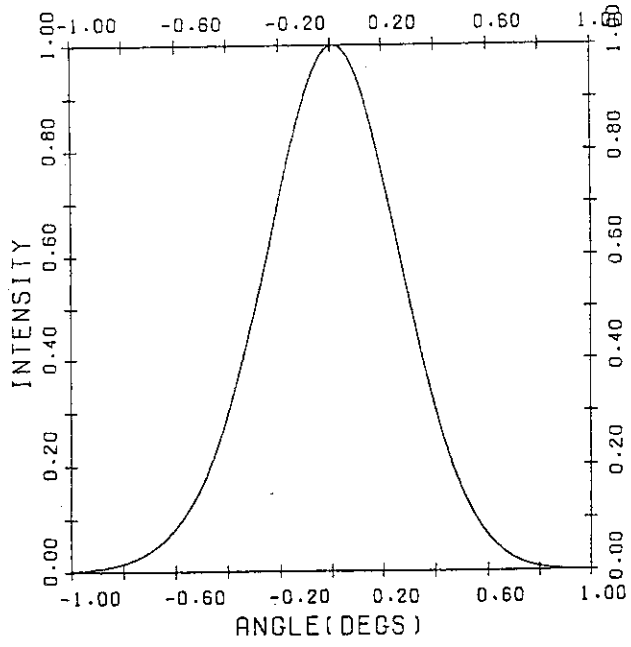

Fig.3-6 Radiation profile of the beam for the injection angle of 20° at the q=2 magnetic surface

Radial distribution of heat deposition

Thickness of Sappire = 1.33 mm

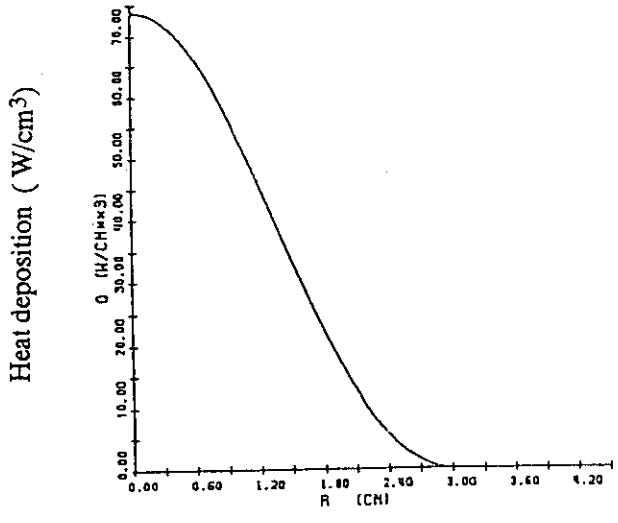

Fig.3-8 Radiation profile of heat deposition due to dielectric heating a the temperature of 77 K

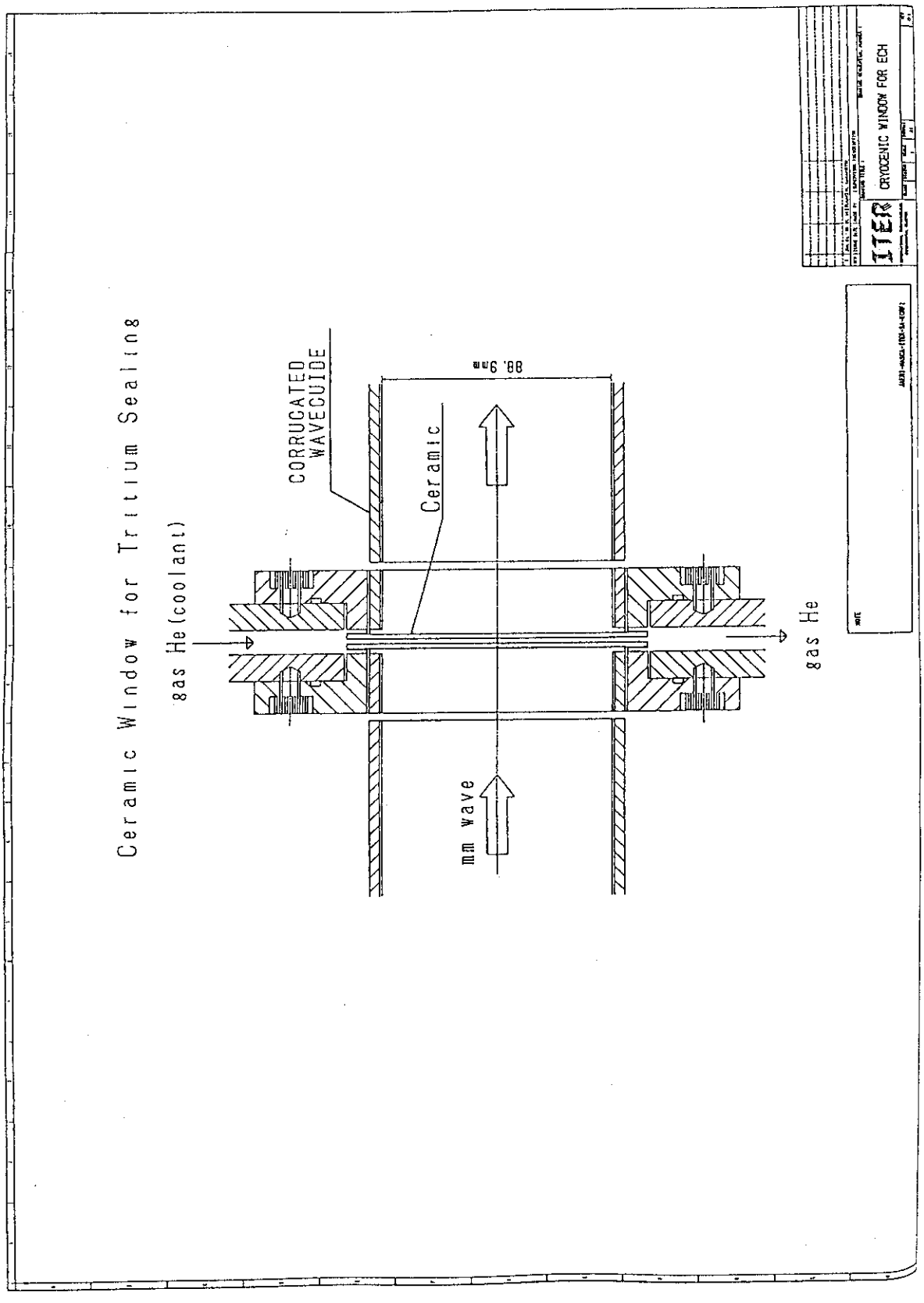

Fig.3-7 Schematic of double disk window

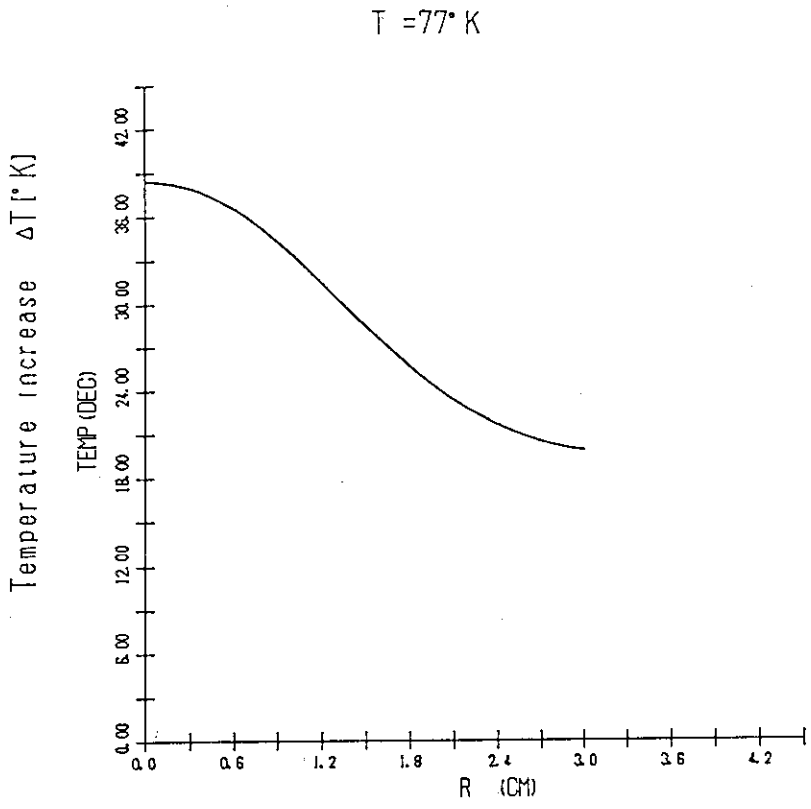

Fig.3-9(a) Radial profiles of increase in the temperature and thermal stress

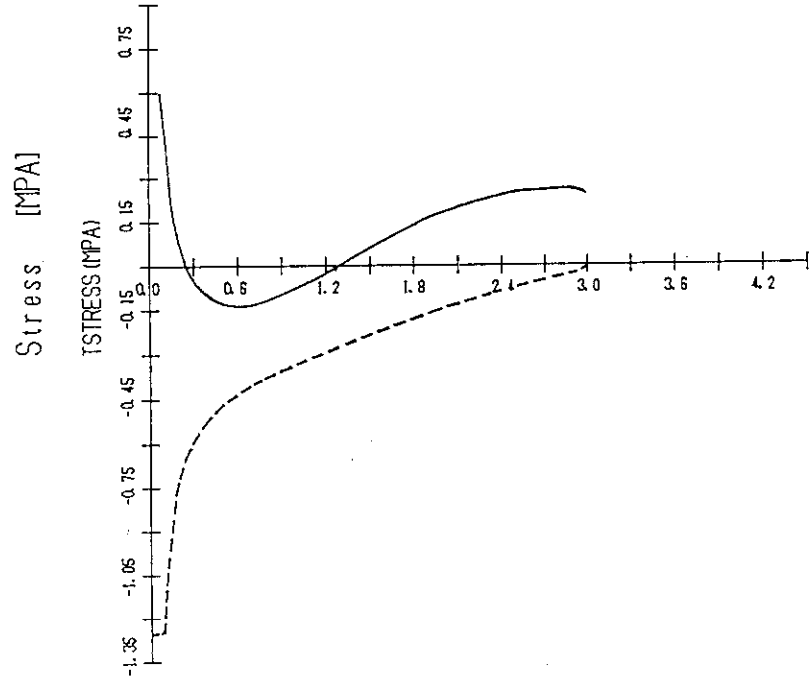

Fig.3-9(b) Radial profiles of increase in the temperature at the initial temperature of 77 K

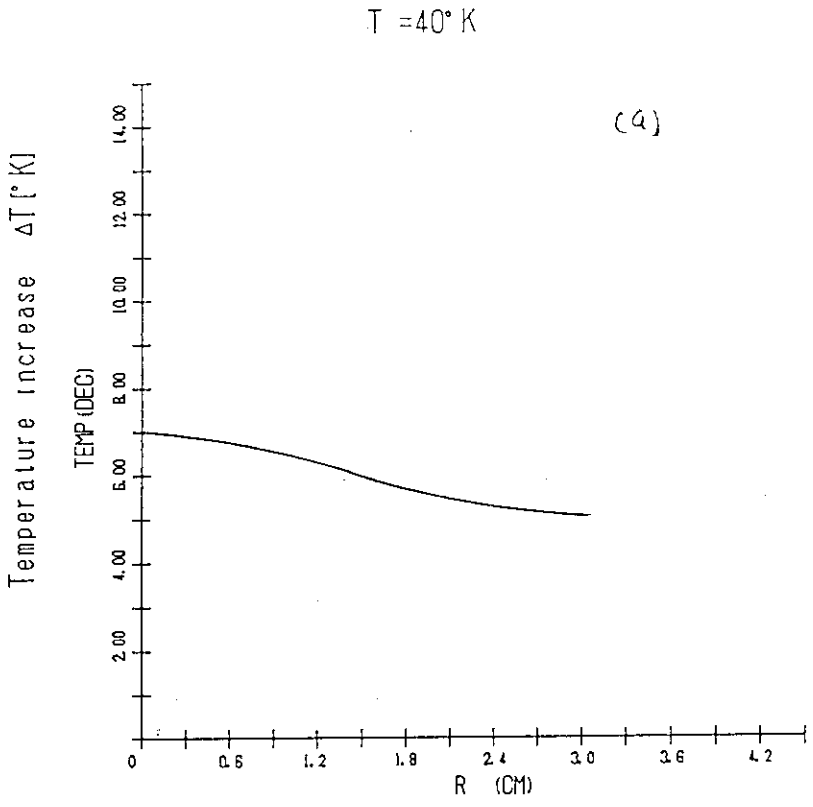

Fig.3-10(a) Radial profiles of increase in the temperature and thermal stress

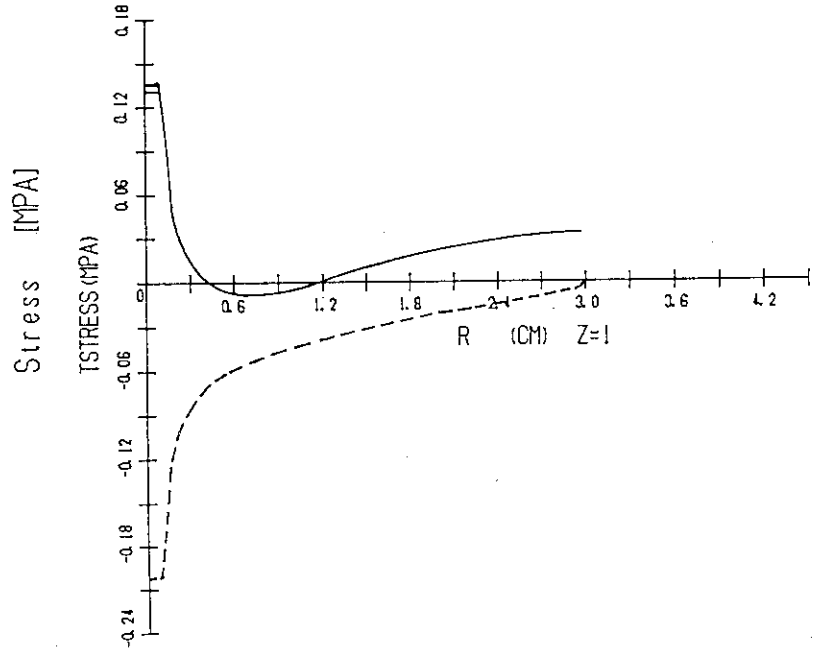

Fig.3-10(b) Radial profiles of increase in the temperature at the initial temperature of 40 K

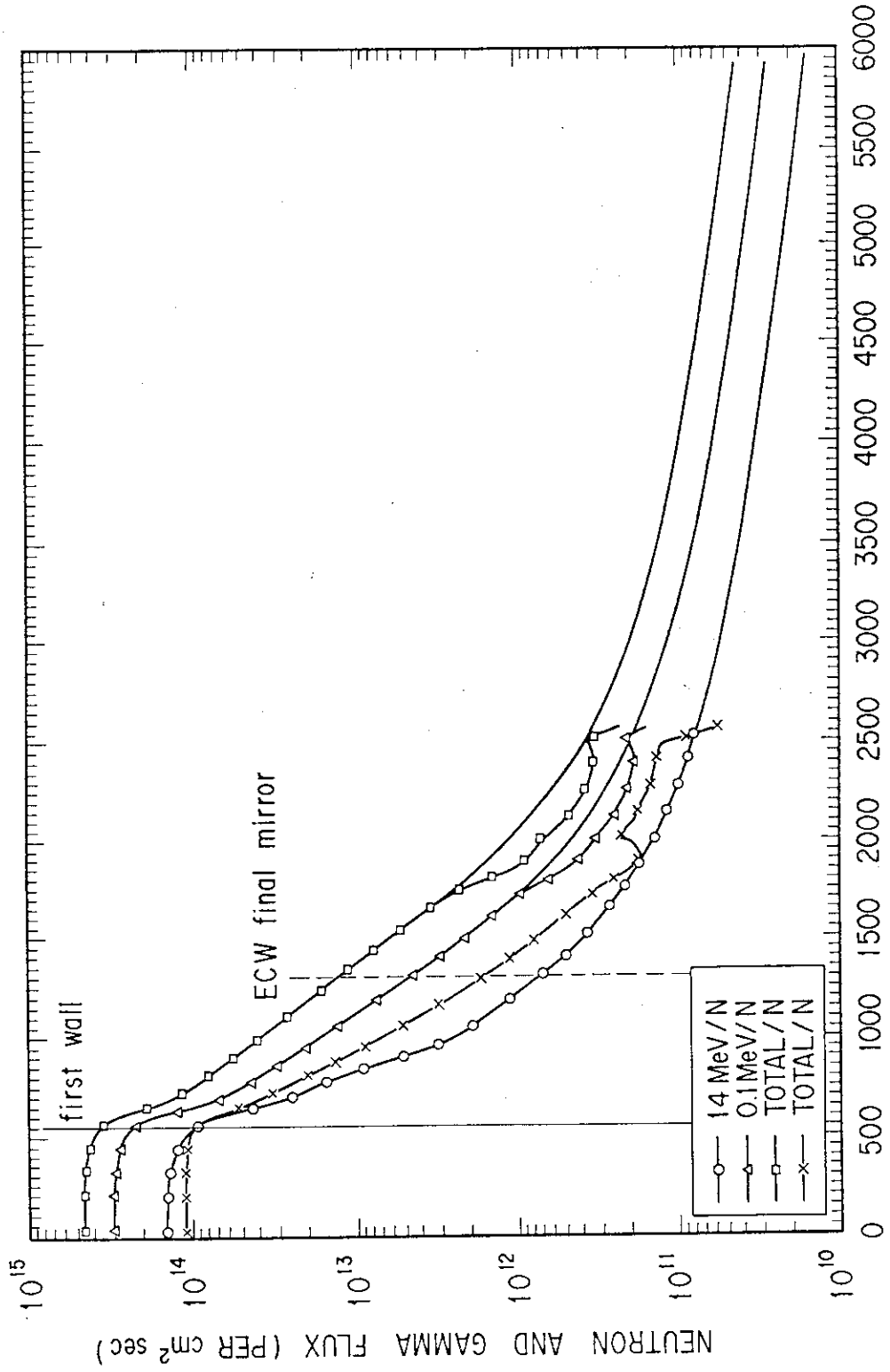

Fig.3-11 Neutron and Gamma ray flux distributions along NBI duct axis

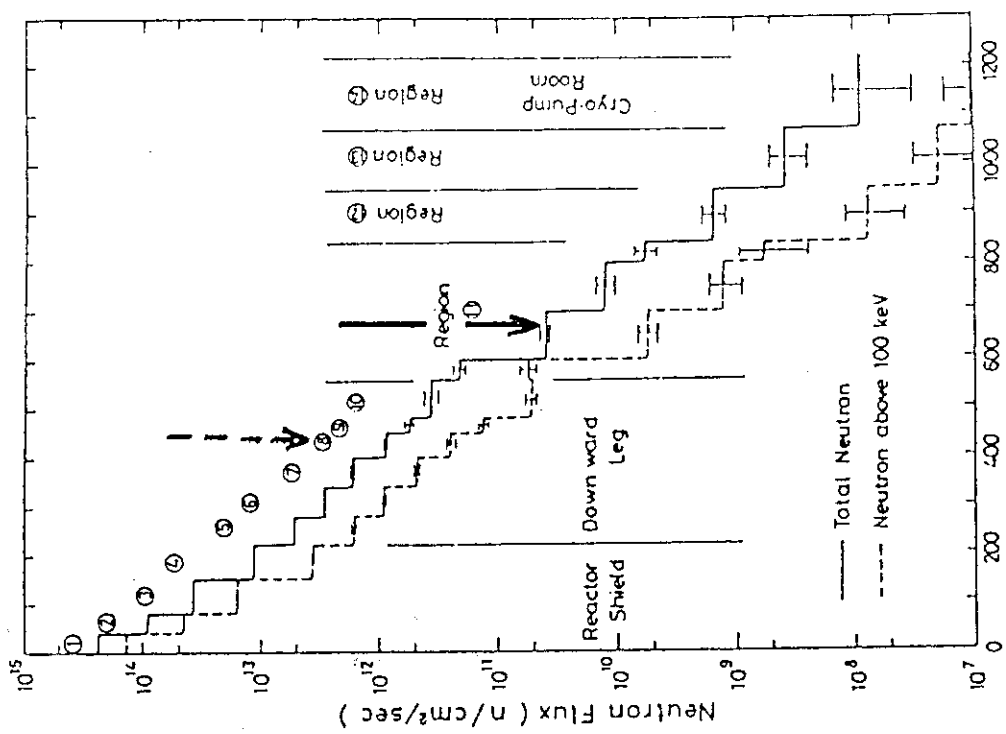

Fig. Neutron Flux Distribution along the Centerline of the RF Duct

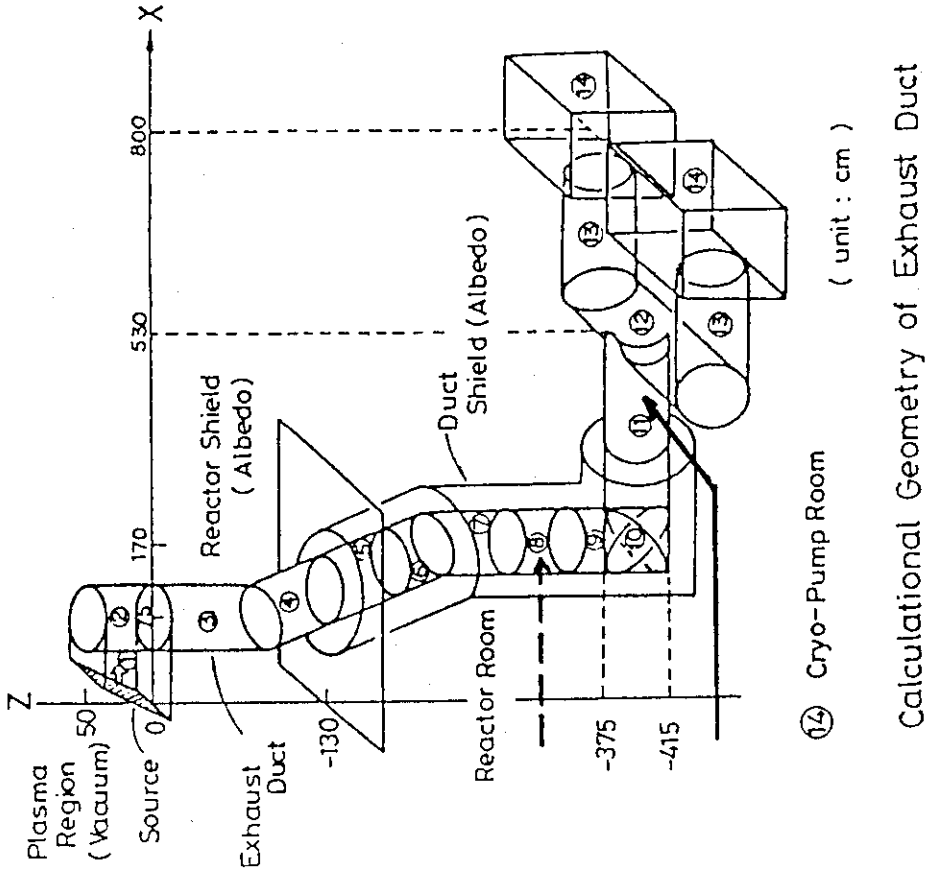

Fig.3-12 Neutron flux distribution along the centerline of the RF duct

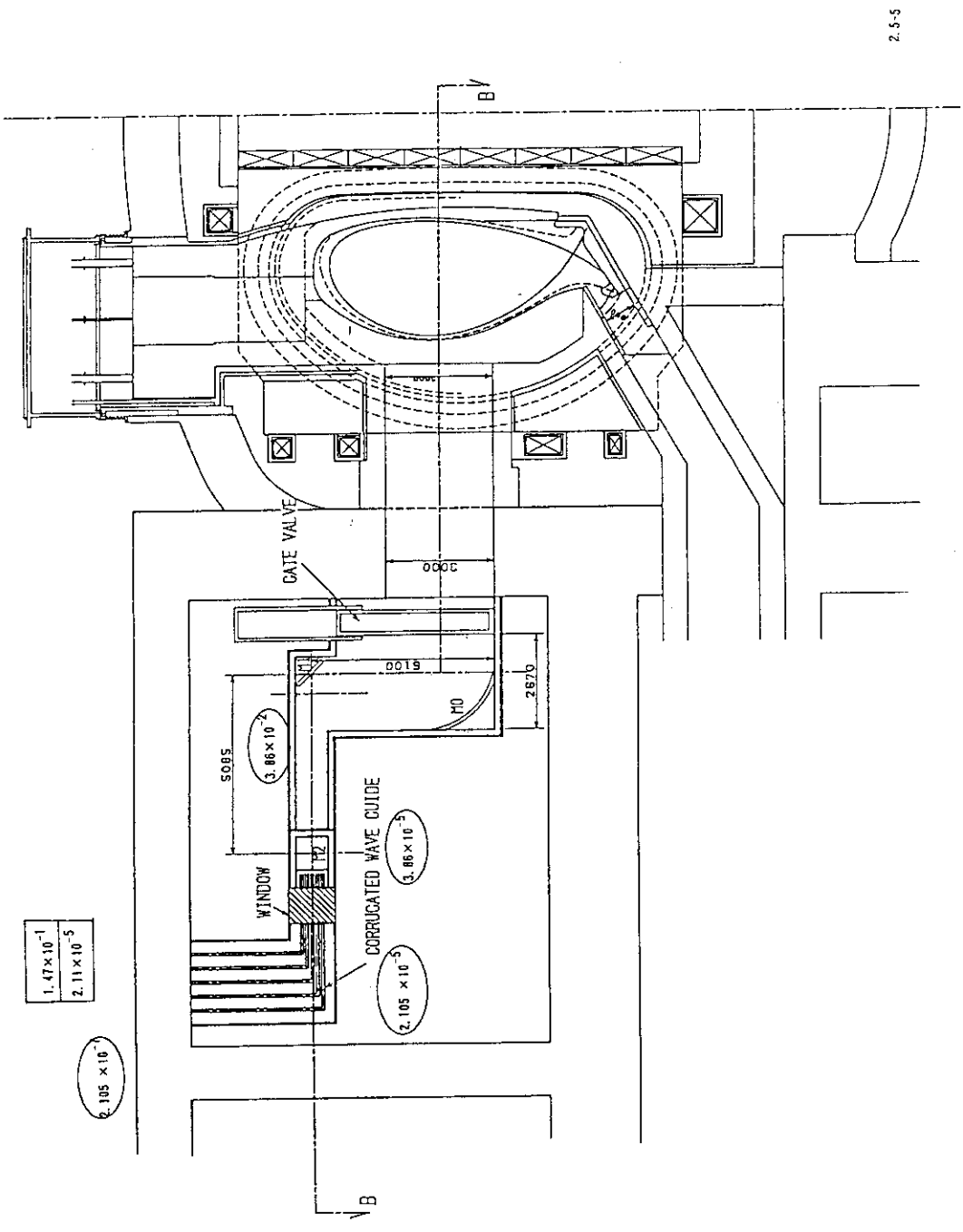

Fig.3-13(a) Neutron shield structure for the launching system: side view.
The number denoted in ellipse indicates the total attenuation rate of neutrons.
The upper and lower numbers in box show a dose of neutron under and after irradiation in mrem/h, respectively.

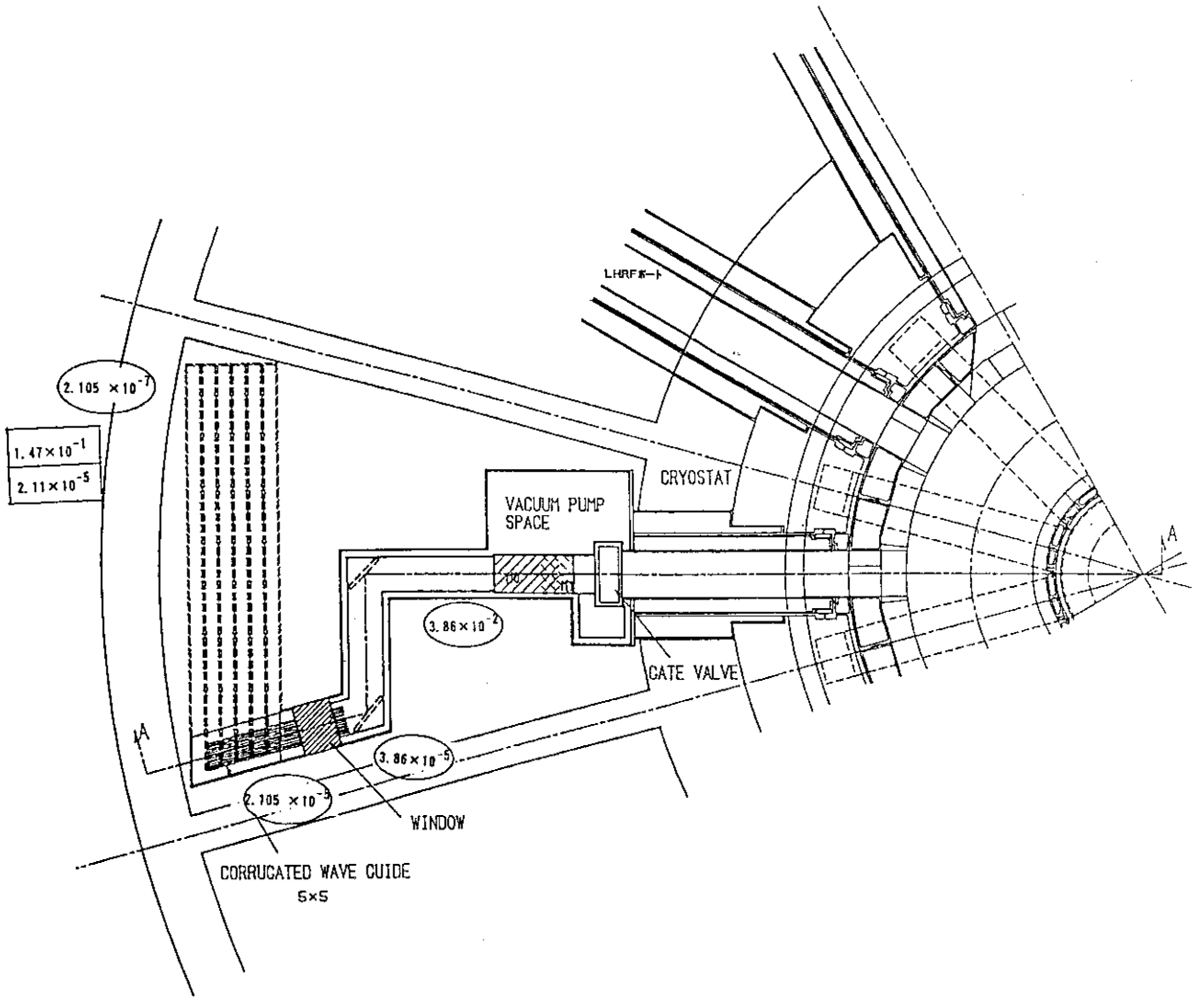

Fig.3-13(b) Neutron shield structure for the launching system: top view.
The number denoted in ellipse indicates the total attenuation rate of neutrons.
The upper and lower numbers in box show a dose of neutron under and after irradiation in mrem/h, respectively.

4.CONCLUSION and FUTURE NEEDS

4.1 R&D needs for FER and ITER

The critical technical issues recognized in CDA for ITER will be studied and planned Long Term Technology R&D should support the engineering design of the EC system. The proposed technology R&D for ITER includes development of the following items. 9) Gyrotron and tokamak windows (cryogenically cooled and advanced concept), 1 MW, CW gyrotron at 120 GHz, transmission line and antenna components specific for the ITER environment, improved mode converter, integrated system test and lifetime tests, support to advanced solution/improvements (gyrotron efficiency enhancement, power supply improvement, gyrotron tunability).

For ITER and Japanese contribution to ITER Long TERM Technical R&D, an emphasis is placed on the development of a high efficiency, 1 MW almost CW (longer than 10 sec) gyrotron at 120 GHz. The higher efficiency of 40 % is planned to be presuaded. Component development on cryogenically cooled window and improved mode converter is under way relating with the component development of the JT-60U EC heating program.

4.2 Conclusions

Further physics studies to support the EC system design are needed in the following areas: (1) experimental investigation of control of the plasma instabilities, (2) optimization of the modeling to define requirements, following FER parameters.

The conceptual design of EC wave system for FER has been carried out. The designed system satisfies the requirement of continuous injection of 20 MW of EC waves at 140 GHz for assist in plasma formation and control of the plasma stabilities and the burn of D-T plasma. An optimization of the physics modeling is necessary as well as the experimental confirmation of theoretical models.

ACKNOWLEDGEMENTS

Authors would like to acknowledge Messrs. N.Furuichi, Y.Iida, Y.Hasegawa, N.Suzuki, K. Hirano, H.Hosobuchi and H.Fujita for skillful and advanced CAD operation.

REFERENCES

1) Matsuda S. et al. : Proc. 13 th Int. Conf. on Plasma Physics and Controlled Nuclear Fusion Research, Washington (1990), IAEA-CN-53/G-2-2.
2) Tomabechi K. et al. : ibid 53/F-1-1.
3) Nevis W. et al. : ibid 53/F-3-4
4) Zarnstorff M. et al. : Phys. Rev. Lett., 60 (1988) 1306.
5) Challis C. et al. :14th Europ. Conf. on Contr. Fusion and Plasma Phys. (Madrid,1987) Part III 1026.
6) Simonen T. et al., : Phys. Rev. Lett. 61 (1988) 1720.
7) JT-60 Team : 16th the Europ. Conf. on Contr. Fusion and Plasma Phys. (Venice,1989)
8) Naito O. et al. : Nucl. Fusion 30 (1990) 1137.
9) Parail V., Fujisawa N., Hopman H., H.Kimura H., et al.: " ITER DOCUMENTATION SERIES, No.32, ITER CURRENT AND HEATING SYSTEM", IAEA, Vienna, 1991.
10) Tsuneoka M. et al., " The Design of RF power Supply Using DC-DC Converter" October 1989 13th SOFE.
11) Haste G.R et al. : ORNL/TM -9906 (1986).
12) Rebuffi L. : " ITER Electron Cyclotron Wave System Common Conceptual Design" (1990)
13) Maki K. et al., : " Japanese Contributions to ITER Shielding Neutronics Design" to be published in JAERI.
14) Yamauchi M., et al. : " The Analysis of the Radiation Streaming through RF Heating and Exhaust Ducts of A Tokamak Fusion Reactor " to be published in JAERI.

ACKNOWLEDGEMENTS

Authors would like to acknowledge Messrs. N.Furuichi, Y.Iida, Y.Hasegawa, N.Suzuki, K. Hirano, H.Hosobuchi and H.Fujita for skillful and advanced CAD operation.

REFERENCES

1) Matsuda S. et al. : Proc. 13 th Int. Conf. on Plasma Physics and Controlled Nuclear Fusion Research, Washington (1990), IAEA-CN-53/G-2-2.
2) Tomabechi K. et al. : ibid 53/F-1-1.
3) Nevis W. et al. : ibid 53/F-3-4
4) Zarnstorff M. et al. : Phys. Rev. Lett., 60 (1988) 1306.
5) Challis C. et al. :14th Europ. Conf. on Contr. Fusion and Plasma Phys. (Madrid,1987) Part III 1026.
6) Simonen T. et al., : Phys. Rev. Lett. 61 (1988) 1720.
7) JT-60 Team : 16th the Europ. Conf. on Contr. Fusion and Plasma Phys. (Venice,1989)
8) Naito O. et al. : Nucl. Fusion 30 (1990) 1137.
9) Parail V., Fujisawa N., Hopman H., H.Kimura H., et al.: " ITER DOCUMENTATION SERIES, No.32, ITER CURRENT AND HEATING SYSTEM", IAEA, Vienna, 1991.
10) Tsuneoka M. et al., " The Design of RF power Supply Using DC-DC Converter" October 1989 13th SOFE.
11) Haste G.R et al. : ORNL/TM -9906 (1986).
12) Rebuffi L. : " ITER Electron Cyclotron Wave System Common Conceptual Design" (1990)
13) Maki K. et al., : " Japanese Contributions to ITER Shielding Neutronics Design" to be published in JAERI.
14) Yamauchi M., et al. : " The Analysis of the Radiation Streaming through RF Heating and Exhaust Ducts of A Tokamak Fusion Reactor " to be published in JAERI.

APPENDIX

Decision of focusing length

1. Because of the finite beam size, the injection angle diverges.

$\delta\theta_1=\delta X/(R\cos\theta)$ $\delta\theta_1$: diverged injection angle of beam 1.

δX : gap between the center beam and beam 1.

2. Compensate the divergence of injection angle by condensing the beam into the tokamak center.

$\delta\theta_2=-\delta X/(R\cos\theta)$

Therefore, total beam divergence is

$\delta\theta=\delta\theta_1+\delta\theta_2=0^\circ$

From the condition 2, the focusing length of mirror 3 and mirror 4 is decided.